

CERN-PH-EP-2012-121

Submitted to: Nuclear Physics B

Measurement of the b -hadron production cross section using decays to $D^{*+}\mu^-X$ final states in pp collisions at $\sqrt{s} = 7$ TeV with the ATLAS detector

The ATLAS Collaboration

Abstract

The b -hadron production cross section is measured with the ATLAS detector in pp collisions at $\sqrt{s} = 7$ TeV, using 3.3 pb^{-1} of integrated luminosity, collected during the 2010 LHC run. The b -hadrons are selected by partially reconstructing $D^{*+}\mu^-X$ final states. Differential cross sections are measured as functions of the transverse momentum and pseudorapidity. The measured production cross section for a b -hadron with $p_T > 9$ GeV and $|\eta| < 2.5$ is 32.7 ± 0.8 (stat.) $^{+4.5}_{-6.8}$ (syst.) μb , higher than the next-to-leading-order QCD predictions but consistent within the experimental and theoretical uncertainties.

Measurement of the b -hadron production cross section using decays to $D^{*+}\mu^-X$ final states in pp collisions at $\sqrt{s} = 7$ TeV with the ATLAS detector

The ATLAS Collaboration

Abstract

The b -hadron production cross section is measured with the ATLAS detector in pp collisions at $\sqrt{s} = 7$ TeV, using 3.3 pb^{-1} of integrated luminosity, collected during the 2010 LHC run. The b -hadrons are selected by partially reconstructing $D^{*+}\mu^-X$ final states. Differential cross sections are measured as functions of the transverse momentum and pseudorapidity. The measured production cross section for a b -hadron with $p_{\text{T}} > 9$ GeV and $|\eta| < 2.5$ is 32.7 ± 0.8 (stat.) $^{+4.5}_{-6.8}$ (syst.) μb , higher than the next-to-leading-order QCD predictions but consistent within the experimental and theoretical uncertainties.

Keywords: QCD, flavour physics, B physics, heavy quark production

1. Introduction

The production of heavy quarks at hadron colliders provides a challenging opportunity to test the validity of quantum chromodynamics (QCD) predictions and calculations. The b -hadron production cross section has been predicted with next-to-leading-order (NLO) accuracy for more than twenty years [1, 2].

Several measurements were performed with proton-antiproton collisions by the UA1 experiment at the Sp \bar{p} S collider (CERN) at a centre-of-mass energy of $\sqrt{s} = 630$ GeV [3, 4], and by the CDF and D0 experiments at the Tevatron collider (Fermilab) at $\sqrt{s} = 630$ GeV, 1.8 TeV and 1.96 TeV [5–14]. These measurements made a significant contribution to the understanding of heavy-quark production in hadronic collisions [15], but the theoretical predictions still suffer from large uncertainties, mainly due to the dependence on the factorisation and renormalisation scales.

A measurement of the b -hadron production cross section in proton-proton collisions at the Large Hadron Collider (LHC) provides a further test of QCD calculations for heavy-quark production at higher centre-of-mass energies. Recently the LHCb experiment measured the $b\bar{b}$ and B^+ [16–18] production cross sections in the forward region at $\sqrt{s} = 7$ TeV, the CMS experiment measured the production cross sections for B^+ , B^0 , B_s^0 mesons, inclusive b -hadrons with muons, and $b\bar{b}$ decays with muons at $\sqrt{s} = 7$ TeV [19–23], and the ALICE experiment measured the $b\bar{b}$ production cross section in pp collisions at $\sqrt{s} = 7$ TeV [24].

This paper presents a measurement of the b -hadron (H_b , a hadron containing a b -quark and not a \bar{b} -quark) production cross section at a centre-of-mass energy of 7 TeV with the

ATLAS detector at the LHC, and its comparison with the NLO QCD theoretical predictions. The measurement requires the partial reconstruction of the b -hadron decay final state $D^{*+}\mu^-X$, with the D^{*+} reconstructed through the fully hadronic decay chain $D^{*+} \rightarrow \pi^+D^0(\rightarrow K^-\pi^+)$. This sample was collected by ATLAS between August and October 2010 using events selected by a single-muon trigger, and corresponds to a total integrated luminosity of 3.3 pb^{-1} .

2. The ATLAS detector

The ATLAS detector [25] covers almost the full solid angle around the collision point with layers of tracking detectors, calorimeters and muon chambers. For the measurement presented in this paper, the inner detector tracking devices, the muon spectrometer and the trigger system are of particular importance.

The inner detector (ID) has full coverage in ϕ and covers the pseudorapidity range $|\eta| < 2.5$. It consists of a silicon pixel detector, a silicon microstrip tracker and a transition radiation tracker composed of drift tubes. These detectors are located at radial distances of 50.5–1066 mm from the interaction point and are surrounded by a thin superconducting solenoid providing a 2 T axial magnetic field. The ID barrel consists of three layers of pixels, four double-layers of single-sided silicon microstrips, and 73 layers of drift tubes, while each ID end-cap has three layers of pixels, nine double-layers of single-sided silicon microstrips, and 160 layers of drift tubes.

The muon spectrometer covers the pseudorapidity range $|\eta| < 2.7$ and is located within the magnetic field produced by three large superconducting air-core toroid systems. The muon spectrometer is divided into a barrel region ($|\eta| < 1.05$) and two end-cap regions ($1.05 < |\eta| < 2.7$), within which the average magnetic fields are 0.5 T and 1 T respectively. Precise measurements are made in the bending plane by monitored drift tube chambers, or, in the innermost layer for $2.0 < |\eta| < 2.7$, by cathode strip chambers. Resistive plate chambers in the barrel and thin gap chambers at $|\eta| < 2.4$ in the end-caps are used as trigger chambers. The chambers are arranged in three layers, such that high p_T muons traverse at least three stations with a lever arm of several metres.

A three-level trigger system is used to select interesting events. The first level is hardware-based, and uses a subset of the detector information to reduce the event rate to a design value of at most 75 kHz. This is followed by two software-based trigger levels, together known as the high level trigger, which finally reduce the event rate to about 200 Hz.

3. Outline of the measurement

The first result presented in this paper is the $H_b \rightarrow D^{*+}\mu^-X$ production cross section, measured in a limited fiducial acceptance for the $D^{*+}\mu^-$ final state. Given the integrated luminosity \mathcal{L} of the data sample, and the branching ratio \mathcal{B} of the D^{*+} cascade decay $D^{*+} \rightarrow \pi^+D^0(\rightarrow K^-\pi^+)$, the $H_b \rightarrow D^{*+}\mu^-X$ cross section is defined as:

$$\sigma(pp \rightarrow H_b X' \rightarrow D^{*+}\mu^-X) = \frac{f_b N(D^{*+}\mu^- + D^{*-}\mu^+)}{2\epsilon\mathcal{B}\mathcal{L}} \quad (1)$$

where $N(D^{*+}\mu^- + D^{*-}\mu^+)$ is the total number of reconstructed candidates, f_b is the fraction of candidates originating from the decay $H_b \rightarrow D^{*+}\mu^- X$ and ϵ is the signal reconstruction efficiency. The efficiency takes into account reconstruction and muon trigger efficiencies, including the loss of events where the D^{*+} falls within the fiducial acceptance, but the decay products (π or K) can not be reconstructed because they fall outside the p_T and η acceptance. The number N of reconstructed candidates includes both $D^{*+}\mu^-$ and $D^{*-}\mu^+$ combinations: assuming that b - and \bar{b} -quarks are produced with the same rate at the LHC, the factor of two is needed to quote the cross section for hadrons containing a b -quark. The value of the branching ratio \mathcal{B} can be obtained by combining the world average values of the branching ratios $D^{*+} \rightarrow \pi^+ D^0$ and $D^0 \rightarrow K^- \pi^+$ [26], and is $(2.63 \pm 0.04)\%$.

The parameters N , f_b and ϵ are determined as functions of the transverse momentum and pseudorapidity of the $D^{*+}\mu^-$ pairs, in order to measure the differential cross sections. The detailed calculation of these parameters is discussed in the following sections.

To obtain the b -hadron production cross section $\sigma(pp \rightarrow H_b X)$, the $H_b \rightarrow D^{*+}\mu^- X$ cross section is divided by an acceptance correction α , accounting for the fiducial region in which this is measured, and by the inclusive branching ratio $\mathcal{B}(b \rightarrow D^{*+}\mu^- X)$. For this branching ratio the world average value is $(2.75 \pm 0.19)\%$, assuming the world average values of the b -hadronisation fractions [26]. The dominant contributions to the sample are from B^0 mesons, through the decay $B^0 \rightarrow D^{*-}\mu^+\nu_\mu$ and its charge conjugate.

4. Event simulation and NLO cross section predictions

Monte Carlo (MC) simulated samples are used to optimise the selection criteria (Section 5) and to evaluate the $D^{*+}\mu^-$ signal composition and reconstruction efficiency (Sections 6 and 7). The different b - and c -quark sources of $D^{*+}\mu^-$ are studied using inclusive samples of $b\bar{b}$ and $c\bar{c}$ events having at least one muon with $p_T > 4$ GeV and $|\eta| < 2.5$ in the final state. Both samples are generated with PYTHIA [27], using the ATLAS AMBT1 tuning [28]. The ATLAS detector response to the passage of the generated particles is simulated with GEANT4 [29, 30], and the simulated events are fully reconstructed with the same software used to process the collision data.

To compare the measurements with theoretical predictions, NLO QCD calculations, matched with a leading-logarithmic parton shower MC simulation, are used. Predictions for $b\bar{b}$ production at the LHC at $\sqrt{s} = 7$ TeV are evaluated with two packages: MC@NLO 4.0 [31, 32] and POWHEG-HVQ 1.01 [33, 34]. MC@NLO is matched with the HERWIG 6.5 [35] MC event generator, while POWHEG is used with both HERWIG 6.5 and PYTHIA 6.4 [27]. For all the predictions, the inclusive branching ratio $\mathcal{B}(b \rightarrow D^{*+}\mu^- X)$ is set to the world average value.

The following set of input parameters is used to perform all theoretical predictions:

- CTEQ6.6 [36] parameterisation for the proton parton distribution function (PDF).
- b -quark mass m_b of 4.75 GeV [26].

- Renormalisation and factorisation scales set to $\mu_r = \mu_f = \mu$, where μ has different definitions for MC@NLO and POWHEG. For MC@NLO:

$$\mu^2 = m_Q^2 + \frac{(p_{T,Q} + p_{T,\bar{Q}})^2}{4}$$

where $p_{T,Q}$ and $p_{T,\bar{Q}}$ are the transverse momenta of the produced heavy quark and antiquark, and m_Q is the heavy-quark mass. For POWHEG:

$$\mu^2 = m_Q^2 + (m_{Q\bar{Q}}^2/4 - m_Q^2) \sin^2(\theta_Q)$$

where $m_{Q\bar{Q}}$ is the invariant mass of the $Q\bar{Q}$ system and θ_Q is the polar angle of the heavy quark in the $Q\bar{Q}$ rest frame.

- Heavy-quark hadronisation: cluster model [37] for HERWIG; Lund string model [38] with Bowler modification [39] of the Lund symmetric fragmentation function [40] for PYTHIA.

The following sources of theoretical uncertainties are included in the NLO predictions:

- Scale uncertainty, determined by varying μ_r and μ_f independently to $\mu/2$ and 2μ , with the additional constraint $1/2 < \mu_r/\mu_f < 2$, and selecting the largest positive and negative variations.
- m_b uncertainty, determined by varying the b -quark mass by ± 0.25 GeV.
- PDF uncertainty, determined by using the CTEQ6.6 PDF error eigenvectors; the total uncertainty is obtained by varying each parameter independently within these errors and summing the resulting variations in quadrature.
- Hadronisation uncertainty, determined in PYTHIA by using the Peterson fragmentation function [41] instead of the Bowler one, with extreme choices of the b -quark fragmentation parameter: $\epsilon_b = 0.002$ and $\epsilon_b = 0.01$.

In addition to the final comparison with the experimental measurement, these theoretical predictions are used to unfold and extrapolate the measured cross sections (Sections 9 and 10), and to extrapolate to the full kinematic phase space (Section 11). In the following, POWHEG+PYTHIA is used as the default prediction.

5. Data selection and reconstruction of the $D^{*+}\mu^-$ decay

The $D^{*+}\mu^-$ (including its charge conjugate) sample was collected during stable proton-proton collisions. Events were selected by a single-muon trigger, which requires a muon, reconstructed by the high level trigger, with $p_T > 6$ GeV. This trigger was prescaled during the last part of the 2010 data-taking period. Taking into account the prescale factors, this data sample corresponds to an integrated luminosity of 3.3 pb^{-1} .

The D^{*+} candidates are reconstructed through the fully hadronic decay chain $D^{*+} \rightarrow \pi^+ D^0 (\rightarrow K^- \pi^+)$, using only good quality tracks, i.e. tracks with at least five silicon detector hits, and at least one of them in the pixel detector.

The b -hadron and D^0 decay vertices are reconstructed and fitted simultaneously. To perform the vertexing, an iterative procedure based on a fast Kalman filtering method is used. This allows to reconstruct consecutively all the vertices of the same decay chain, using the full information from track reconstruction (particles trajectories with complete error matrices). All pairs of opposite charge particle tracks are fitted to a single vertex to form D^0 candidates, assigning to each track, in turn, the kaon or the pion mass, with the additional requirement $p_T > 1$ GeV for both the kaon and pion candidate; the resulting D^0 candidate is reconstructed by combining the kaon and pion four-momenta. The D^0 path is then extrapolated back and fitted with a track of opposite charge to the candidate kaon, requiring $p_T > 250$ MeV and assigning to it the pion mass, to form the D^{*+} candidate, and with a muon with $p_T > 6$ GeV and $|\eta| < 2.4$ to form the b -hadron vertex. No requirements are made here on the muon charge; only opposite charge combinations $D^{*+} \mu^-$ are used in the analysis, while same charge combinations are used to cross-check the background. The muon is also required to have fired the trigger. To ensure good fit quality, the global χ^2 probability of the combined fit must satisfy $P(\chi^2) > 0.001$. To avoid an additional systematic uncertainty no requirement on the b -hadron vertex decay length is applied.

The D^{*+} candidate is accepted if it satisfies $p_T(K^- \pi^+ \pi^+) > 4.5$ GeV and $|\eta(K^- \pi^+ \pi^+)| < 2.5$, and either (a) $|m(K^- \pi^+) - m(D^0)| < 64$ MeV in the region $p_T(K^- \pi^+ \pi^+) > 12$ GeV and $|\eta(K^- \pi^+ \pi^+)| > 1.3$, or (b) $|m(K^- \pi^+) - m(D^0)| < 40$ MeV elsewhere. Here $m(D^0)$ is the world average value for the D^0 mass [26]. This last selection cut is divided into two different kinematic regions due to the changing D^0 mass resolution. The $D^{*+} \mu^-$ candidate must have an invariant mass in the range 2.5–5.4 GeV. The upper invariant mass cut matches the physical requirement of not exceeding the mass of the B -mesons.

Because of the kinematics of the D^{*+} decay, the prompt pion takes only a small fraction of the energy. The D^{*+} signal is therefore studied as a function of the mass difference Δm between the D^{*+} and D^0 candidates. Real D^{*+} mesons are expected to form a peak in Δm around 145.4 MeV, while the combinatorial background gives a rising distribution, starting at the pion mass. The combinatorial background is made of fake $D^{*+} \mu^-$ candidates, created from combinations of tracks which pass the selection cuts, but do not come from a $D^{*+} \mu^-$ signal. Figure 1 (a) shows a clear signal in the distribution of Δm for the reconstructed opposite charge $D^* \mu$ pairs. The dashed histogram shows the corresponding Δm distribution for the same charge combinations $D^{*\pm} \mu^\pm$, showing a very small excess around 145.4 MeV, whose origin is described in Section 6.

The opposite charged signal distribution is fitted using a modified Gaussian (G^{mod}), which provides a good description of the tails of the signal distribution. The modified Gaussian has the form:

$$G^{\text{mod}}(x) \propto \exp[-0.5 \cdot x^{1+\frac{1}{1+0.5x}}] \quad (2)$$

where $x = |(\Delta m - \Delta m_0)/\sigma|$ and Δm_0 and σ , free parameters in the fit, are the mean and width of the Δm peak.

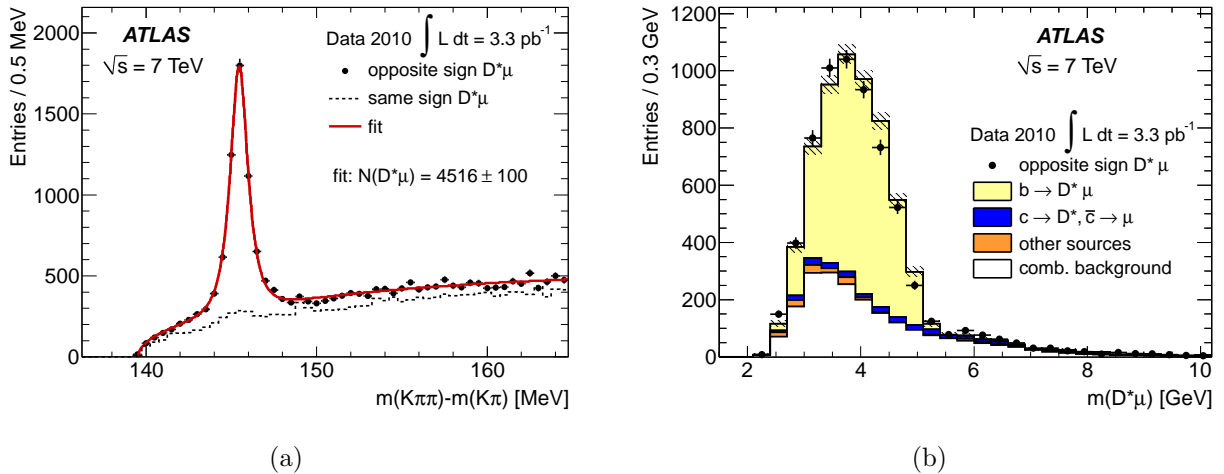


Figure 1: (a) Distribution of the mass difference Δm for $D^*\mu$ combinations of opposite charge (points) and same charge (dashed line). The solid line shows the result of the fit described in the text. (b) Distribution of the opposite charge $D^*\mu$ invariant mass, for mass combinations within $\pm 3\sigma$ of the Δm peak, without applying the invariant mass cut described in the text. The measured distribution is compared with the MC simulation, including the contribution of different sources of signal. The hashed bands show the MC statistical uncertainty.

The combinatorial background is fitted with a power function multiplied by an exponential function:

$$B(\Delta m) \propto (\Delta m - m_\pi)^\alpha e^{-\beta(\Delta m - m_\pi)} \quad (3)$$

where α and β are free fit parameters, and m_π is the charged pion mass.

The fitted yield is 4516 ± 100 events, with a fitted $\Delta m_0 = 145.463 \pm 0.015$ MeV, to be compared with the world average value 145.421 ± 0.010 MeV [26], and a fitted $\sigma = 0.49 \pm 0.03$ MeV. The uncertainties on the fitted Δm_0 and σ values are statistical only.

Figure 1 (b) shows the $D^{*+}\mu^-$ invariant mass distribution selected in a region of 3σ around the Δm peak, without applying any $D^{*+}\mu^-$ invariant mass cut. The measured distribution is compared with the MC $b\bar{b} + c\bar{c}$ simulation described in Section 4, which takes into account the contribution of different physical sources to the $D^{*+}\mu^-$ signal, as discussed in more detail in Section 6. The MC simulation is separately normalised to the number of signal and background events in data. The selection on $m(D^{*+}\mu^-)$ has full efficiency for the signal, while rejecting part of the combinatorial background and physical processes other than a single b -hadron decay.

In order to evaluate differential cross sections, the sample is divided into six $p_T(D^{*+}\mu^-)$ bins and five $|\eta(D^{*+}\mu^-)|$ bins. The Δm distribution in each bin is fitted independently using the same fitting procedure as for the total sample. The number of candidates in each bin is reported in Table 1, together with its statistical uncertainty from the fit.

6. $D^{*+}\mu^-$ sample composition

Various processes contribute to the $D^{*+}\mu^-$ data sample:

$p_T(D^{*+}\mu^-)$	$N(D^{*+}\mu^-)$	$ \eta(D^{*+}\mu^-) $	$N(D^{*+}\mu^-)$
9–12 GeV	334 ± 33	0.0–0.5	1330 ± 47
12–15 GeV	1211 ± 56	0.5–1.0	1207 ± 47
15–20 GeV	1527 ± 55	1.0–1.5	919 ± 48
20–30 GeV	1049 ± 42	1.5–2.0	890 ± 60
30–45 GeV	310 ± 21	2.0–2.5	317 ± 37
45–80 GeV	76 ± 10		

Table 1: Fitted number of opposite charge $D^*\mu$ pairs for different p_T and $|\eta|$ bins.

- Direct semileptonic decay: $b \rightarrow D^{*+}\mu^-X$; this is the signal contribution used for this measurement.
- Decays of two c -hadrons, one of them decaying semileptonically: $c \rightarrow D^{*+}X$, $\bar{c} \rightarrow \mu^-X'$.
- Direct semileptonic τ decay: $b \rightarrow D^{*+}\tau^-X$, $\tau^- \rightarrow \mu^-\bar{\nu}_\mu\nu_\tau(\gamma)$.
- Decays of b -hadrons with two c -hadrons in the final state, one of them decaying semileptonically: $b \rightarrow D^{*+}\bar{D}X$, $\bar{D} \rightarrow \mu^-X'$.
- Decays of two b -hadrons, one of them decaying semileptonically: $b \rightarrow D^{*+}X$, $\bar{b} \rightarrow \mu X'$. This source contributes to opposite-sign and same-sign charge combinations, depending on the direct or indirect semileptonic decay relative branching ratio and on the neutral b -meson oscillation rate. This explains the small excess observed in Figure 1 (a) in the peak region of the same sign charge Δm distribution.
- A D^{*+} meson accompanied by a fake muon, contributing to both opposite-sign and same-sign charge combinations. The contribution from combinations with misidentified muon charge is negligible.

For the purposes of this measurement, only the direct semileptonic component is of interest. Therefore it is necessary to evaluate the fraction of the reconstructed $D^{*+}\mu^-$ sample that actually originates from direct semileptonic b decays. This is estimated from the MC simulation. The most significant $D^{*+}\mu^-$ contributions are listed in Table 2, together with the MC statistical uncertainty.

The fractions from single b semileptonic decays f_b , evaluated in the various p_T and $|\eta|$ bins of the $D^{*+}\mu^-$ pair, are reported in Table 3, together with the MC statistical uncertainty of the calculations. These values are used for the differential cross section measurements.

7. Reconstruction and muon trigger efficiency

The overall efficiency ϵ for $H_b \rightarrow D^{*+}\mu^-X$ decays to enter the $D^{*+}\mu^-$ sample, which includes the reconstruction, muon trigger and selection efficiencies, is evaluated as a product

Source	Fraction (%)
$b \rightarrow D^{*+}\mu^- X$	93.2 ± 0.3
$c \rightarrow D^{*+} X, \bar{c} \rightarrow \mu^- X'$	3.8 ± 0.2
$b \rightarrow D^{*+}\tau^- X, \tau^- \rightarrow \mu^- X'$	1.5 ± 0.1
$b \rightarrow D^{*+}\bar{D} X, \bar{D} \rightarrow \mu^- X'$	0.9 ± 0.1
others	0.6 ± 0.1

Table 2: Different sources contributing to the $D^{*+}\mu^-$ sample. The uncertainties are due to MC statistics.

$p_T(D^{*+}\mu^-)$	f_b (%)	$ \eta(D^{*+}\mu^-) $	f_b (%)
9–12 GeV	90.8 ± 1.2	0.0–0.5	93.0 ± 0.5
12–15 GeV	92.7 ± 0.5	0.5–1.0	92.6 ± 0.5
15–20 GeV	93.8 ± 0.4	1.0–1.5	93.4 ± 0.6
20–30 GeV	93.2 ± 0.5	1.5–2.0	93.5 ± 0.6
30–45 GeV	93.8 ± 0.9	2.0–2.5	94.6 ± 0.9
45–80 GeV	93.1 ± 1.9		

Table 3: Fractions of single b semileptonic decays in different $p_T(D^{*+}\mu^-)$ and $|\eta(D^{*+}\mu^-)|$ bins. The uncertainties are due to MC statistics.

of three different components, in order to combine MC and data-driven efficiency calculations. Since the only requirement is the single b detection efficiency, the $b\bar{b}$ MC sample is used. The components are defined as:

$$\epsilon_{\text{reco}} = \frac{N(\text{true } D^{*+}\mu^- \text{ with } \mu \text{ and tracks reconstructed})}{N(\text{true } D^{*+}\mu^-)} \quad (4)$$

$$\epsilon_{\text{trigger}} = \frac{N(\text{true } D^{*+}\mu^- \text{ with } \mu \text{ and tracks reconstructed, } \mu \text{ matched to trigger})}{N(\text{true } D^{*+}\mu^- \text{ with } \mu \text{ and tracks reconstructed})} \quad (5)$$

$$\epsilon_{\text{selection}} = \frac{N(\text{true } D^{*+}\mu^- \text{ with } \mu \text{ and tracks rec., } \mu \text{ matched to trigger, } D^{*+}\mu^- \text{ selection})}{N(\text{true } D^{*+}\mu^- \text{ with } \mu \text{ and tracks rec., } \mu \text{ matched to trigger})} \quad (6)$$

where the number of true $D^{*+}\mu^-$ pairs is calculated within the fiducial kinematic region $p_T(D^{*+}) > 4.5$ GeV, $p_T(\mu^-) > 6$ GeV, $|\eta(D^{*+})| < 2.5$ and $|\eta(\mu^-)| < 2.4$. Events where the D^{*+} is inside the fiducial region, but its decay products are not fully reconstructed, contribute to ϵ_{reco} .

Both ϵ_{reco} and $\epsilon_{\text{selection}}$ are taken from MC simulation. However $\epsilon_{\text{trigger}}$, which is the fraction of the reconstructed muons that actually satisfied the trigger, is measured directly from data using $J/\psi \rightarrow \mu^+\mu^-$ samples [42]. These efficiencies are evaluated for the same data-taking periods used in this measurement.

The overall efficiency ϵ is given by:

$$\epsilon = \epsilon_{\text{reco}}(\text{MC})\epsilon_{\text{trigger}}(\text{data})\epsilon_{\text{selection}}(\text{MC}) \quad (7)$$

The different efficiency components, together with the related statistical uncertainties, are determined as $\epsilon_{\text{reco}} = (48.3 \pm 0.4)\%$, $\epsilon_{\text{trigger}} = (81.9 \pm 0.4)\%$ and $\epsilon_{\text{selection}} = (79.1 \pm 0.5)\%$. The overall efficiency is $(31.3 \pm 0.4)\%$, and the values obtained in $p_{\text{T}}(D^{*+}\mu^-)$ and $|\eta(D^{*+}\mu^-)|$ bins are reported in Table 4. A complete description of the systematic uncertainties follows in Section 8.

$p_{\text{T}}(D^{*+}\mu^-)$	ϵ (%)	$ \eta(D^{*+}\mu^-) $	ϵ (%)
9–12 GeV	21.2 ± 0.9	0.0–0.5	37.5 ± 0.7
12–15 GeV	26.7 ± 0.6	0.5–1.0	37.2 ± 0.8
15–20 GeV	32.1 ± 0.6	1.0–1.5	29.9 ± 0.8
20–30 GeV	38.8 ± 0.9	1.5–2.0	26.1 ± 0.8
30–45 GeV	45.2 ± 1.7	2.0–2.5	16.1 ± 0.9
45–80 GeV	52 ± 4		

Table 4: Overall efficiency ϵ for different $p_{\text{T}}(D^{*+}\mu^-)$ and $|\eta(D^{*+}\mu^-)|$ bins.

8. Systematic uncertainties

The uncertainty in the cross section due to each systematic variation is evaluated by repeating the entire analysis procedure and finding the change in the cross section value. The same strategy is adopted to evaluate bin-by-bin systematic uncertainties for the differential cross section measurements. The following sources are considered:

- Uncertainty of the yields from the fits, obtained by varying the fitting procedure in the following ways:
 - reducing the high end of the Δm range used for the $D^{*+}\mu^-$ signal fit by 4 MeV, from 165 MeV to 161 MeV;
 - changing the background parameterisation function to be $\propto 1 - \exp(-\alpha(\Delta m - m_{\pi})^{\beta})$, where α and β are free fit parameters, which provides a $P(\chi^2)$ for the fit similar to that with the default background parameterisation.
- Uncertainty of the sample composition estimate: the f_b measurement depends on the b/c cross section ratio used in the MC sample. The ratio of the beauty and charm contributions to the inclusive D^{*+} production, estimated using the life-time information, has been found to be in agreement with the ratio in PYTHIA, within experimental uncertainties. To cover the uncertainties, the MC b/c ratio is varied between 50% and 200% of its nominal value.
- Uncertainties of the muon trigger efficiencies are estimated from $J/\psi \rightarrow \mu^+\mu^-$ studies [42].

- Uncertainty on tracking and muon reconstruction efficiency: the uncertainty on ID tracking efficiency is dominated by the detector material description used in MC simulations. This uncertainty is evaluated in studies of minimum bias events [28]. The muon reconstruction uncertainty is evaluated on $Z \rightarrow \mu^+\mu^-$ data samples [42]. This systematic uncertainty is dominated by the ID tracking uncertainty.
- Model dependence of the reconstruction efficiency: the efficiency calculation could be affected by differences between the $p_T(D^{*+}\mu^-)$ and $\eta(D^{*+}\mu^-)$ spectra in data and MC simulation. To estimate the systematic uncertainty, the MC distribution is varied, while preserving consistency with the observed data distribution, and the resulting change in efficiency is computed after each variation.
- Uncertainty due to differences in the fit of the D^0 and b -hadron vertices between data and MC simulation: to estimate the systematic uncertainty, the MC $P(\chi^2)$ distribution is varied, while preserving consistency with the observed data distribution, and the resulting change in efficiency is computed after each variation.
- Uncertainty of the difference in D^0 mass resolution between data and MC simulation: the efficiency calculation is corrected to account the difference between D^0 mass resolution in data and MC simulation. To estimate the systematic uncertainty, the error on the data-to-MC ratio of D^0 mass widths is propagated to the efficiency.
- NLO prediction uncertainty: since the NLO predictions are also used as an active part of the analysis for unfolding (Section 9) and acceptance corrections (Section 10), the theoretical uncertainties and the use of different predictions introduce additional systematic uncertainties to the experimental measurements. These are evaluated by repeating the entire analysis, introducing different theoretical uncertainties (Section 4) to the default central prediction (POWHEG+PYTHIA), and using a different theoretical prediction (POWHEG+HERWIG and MC@NLO): positive and negative differences obtained with respect to using the central prediction are separately summed in quadrature. The use of the predictions matched with HERWIG produces visible asymmetries in the uncertainties of the acceptance corrections (Section 10).
- Uncertainty of the luminosity measurement ($\pm 3.4\%$)[43, 44].
- Relative uncertainty on the branching fractions of the different decay chains, obtained from the world averages [26]: $b \rightarrow D^{*+}\mu^- X$ ($\pm 7\%$), $D^{*+} \rightarrow D^0\pi^+$ ($\pm 0.7\%$), $D^0 \rightarrow K^-\pi^+$ ($\pm 1.3\%$).

In Sections 9 and 10, tables are shown with these uncertainties quoted after each step of the analysis.

9. Differential cross sections for $H_b \rightarrow D^{*+}\mu^- X$ production

Differential cross sections for $H_b \rightarrow D^{*+}\mu^- X$ production as a function of the p_T and $|\eta|$ of the $D^{*+}\mu^-$ pairs are evaluated by using Equation 1 and dividing by the bin width. The results are shown in Table 5.

$p_T(D^{*+}\mu^-)$ [GeV]	$\frac{d\sigma(H_b \rightarrow D^{*+}\mu^- X)}{dp_T(D^{*+}\mu^-)}$ [nb/GeV]	$ \eta(D^{*+}\mu^-) $	$\frac{d\sigma(H_b \rightarrow D^{*+}\mu^- X)}{d \eta(D^{*+}\mu^-) }$ [nb/unit of $ \eta $]
9–12	$2.78 \pm 0.29^{+0.30}_{-0.30}$	0.0–0.5	$38.4 \pm 1.5^{+3.4}_{-3.4}$
12–15	$8.2 \pm 0.4^{+0.8}_{-0.8}$	0.5–1.0	$34.9 \pm 1.4^{+3.1}_{-3.1}$
15–20	$5.2 \pm 0.2^{+0.5}_{-0.5}$	1.0–1.5	$33.5 \pm 1.8^{+3.4}_{-3.1}$
20–30	$1.47 \pm 0.06^{+0.15}_{-0.14}$	1.5–2.0	$37.2 \pm 2.6^{+4.7}_{-4.2}$
30–45	$0.250 \pm 0.018^{+0.025}_{-0.024}$	2.0–2.5	$21.7 \pm 2.6^{+3.7}_{-3.1}$
45–80	$0.0229 \pm 0.0030^{+0.0023}_{-0.0023}$		

Table 5: Differential cross sections for $H_b \rightarrow D^{*+}\mu^- X$ production as a function of p_T and $|\eta|$ of the $D^{*+}\mu^-$ pair, in the fiducial kinematical region $p_T(D^{*+}) > 4.5$ GeV, $p_T(\mu^-) > 6$ GeV, $|\eta(D^{*+})| < 2.5$ and $|\eta(\mu^-)| < 2.4$. The statistical and total systematic uncertainties are shown for each cross section.

To extract differential cross sections as a function of the p_T and $|\eta|$ of the b -hadron, it is necessary to correct the observed $p_T(D^{*+}\mu^-)$ and $|\eta(D^{*+}\mu^-)|$ distributions using Monte Carlo simulations, in order to take into account the kinematics of the missing particles from the decay $H_b \rightarrow D^{*+}\mu^- X$. This procedure is known as unfolding [45–48]. The unfolding approach used in this paper is based on the iterative method described in Ref. [49], containing elements of Bayesian statistics.

The element F_{ij} of the response matrix F for a b -hadron in a $p_T/|\eta|(H_b)$ bin j to decay into a $D^{*+}\mu^-$ in $p_T/|\eta|(D^{*+}\mu^-)$ bin i can be interpreted as a conditional probability

$$F_{ij} = P(D^{*+}\mu^- \text{ in bin } i | H_b \text{ in bin } j). \quad (8)$$

Given an initial set of probabilities p_i for b -hadrons to be found in bin i , using Bayes' theorem one can obtain the expected number of b -hadrons in bin i , given a measured $D^{*+}\mu^-$ distribution:

$$N_i^{H_b} = \sum_{j=1}^{N_{\text{bin}}} P(H_b \text{ in bin } i | D^{*+}\mu^- \text{ in bin } j) N_j^{D^{*+}\mu^-} = \sum_{j=1}^{N_{\text{bin}}} \left(\frac{F_{ji} p_j}{\sum_k F_{jk} p_k} \right) N_j^{D^{*+}\mu^-}. \quad (9)$$

A NLO Monte Carlo sample generated with POWHEG+PYTHIA is used to create the default response matrix F and the initial prior probabilities p . The procedure is repeated with different MC generators, in order to evaluate systematic uncertainties.

The procedure can be iterated, taking as new prior probabilities the solutions of the previous step, i.e. $p_i = N_i^{H_b} / N_{\text{tot}}^{H_b}$. After a large number of iterations, the procedure converges

on the results obtained with a direct inversion of the response matrix F

$$N_i^{H_b} = \sum_{j=1}^{N_{\text{bin}}} (F^{-1})_{ij} N_j^{D^{*+}\mu^-}. \quad (10)$$

This method is known to be sensitive to statistical fluctuations [45], but this effect can be mitigated in the Bayesian method by truncating the procedure after a few iterations.

The number of iterations was therefore optimised in Monte Carlo simulations with test measurements, comparing the values obtained after each iteration to the values expected from the MC-generated information, using a χ^2 test. Two iterations are the optimal solution in this case, providing compatible results even when the response matrix F and the prior probabilities p are generated using different theoretical distributions.

The inversion method and the Bayesian method with a different number of iterations were employed as a check. Within the systematic uncertainties, all the results were found to be in agreement with the chosen default procedure.

A bias could occur in this procedure due to the possible mismodelling of the H_b decays (e.g. D^{**} decays contributing to the missing particles in the final state) in the simulation. It was verified with the simulation that the relevant $D^{*+}\mu^-$ kinematic variables have a small dependence on the specific b -hadron decay, and that a mismodelling of the D^{**} branching ratios does not produce a significant effect. This is expected since the dominant $D^{*+}\mu^-$ contribution arises from direct B^0 decays without an intermediate D^{**} .

Once the H_b distribution is obtained, the differential $H_b \rightarrow D^{*+}\mu^- X$ cross sections are determined as a function of p_T and $|\eta|$ of the b -hadron, inside the kinematic region $p_T(D^{*+}) > 4.5$ GeV, $p_T(\mu^-) > 6$ GeV, $|\eta(D^{*+})| < 2.5$ and $|\eta(\mu^-)| < 2.4$.

Figure 2 shows the measured differential cross sections, with comparisons to the NLO theoretical predictions. The POWHEG+PYTHIA shaded band refers to the total theoretical uncertainty of the prediction. The differential cross section values are reported in Table 6, together with the statistical and total systematic uncertainties. The individual contributions to the systematic uncertainties are listed in Tables 7 and 8. The comparison with data shows that NLO calculations underestimate the cross section, although the difference is within the combined experimental and theoretical uncertainties.

The integrated $H_b \rightarrow D^{*+}\mu^- X$ cross section, inside the kinematic region $p_T(D^{*+}) > 4.5$ GeV, $p_T(\mu^-) > 6$ GeV, $|\eta(D^{*+})| < 2.5$ and $|\eta(\mu^-)| < 2.4$, is:

$$\sigma(pp \rightarrow H_b X' \rightarrow D^{*+}\mu^- X) = 78.7 \pm 2.0 \text{ (stat.)} \pm 7.3 \text{ (syst.)} \pm 1.2(\mathcal{B}) \pm 2.7(\mathcal{L}) \text{ nb}$$

The integrated POWHEG+PYTHIA prediction, with its theoretical uncertainty, is:

$$\sigma(pp \rightarrow H_b X' \rightarrow D^{*+}\mu^- X) = 53_{-12}^{+18}(\text{scale})_{-3}^{+3}(m_b)_{-3}^{+3}(\text{PDF})_{-5}^{+6}(\text{hadr.}) \text{ nb}$$

The corresponding POWHEG+HERWIG prediction is 51 nb, while MC@NLO predicts 56 nb, with similar theoretical uncertainties to the POWHEG+PYTHIA prediction.

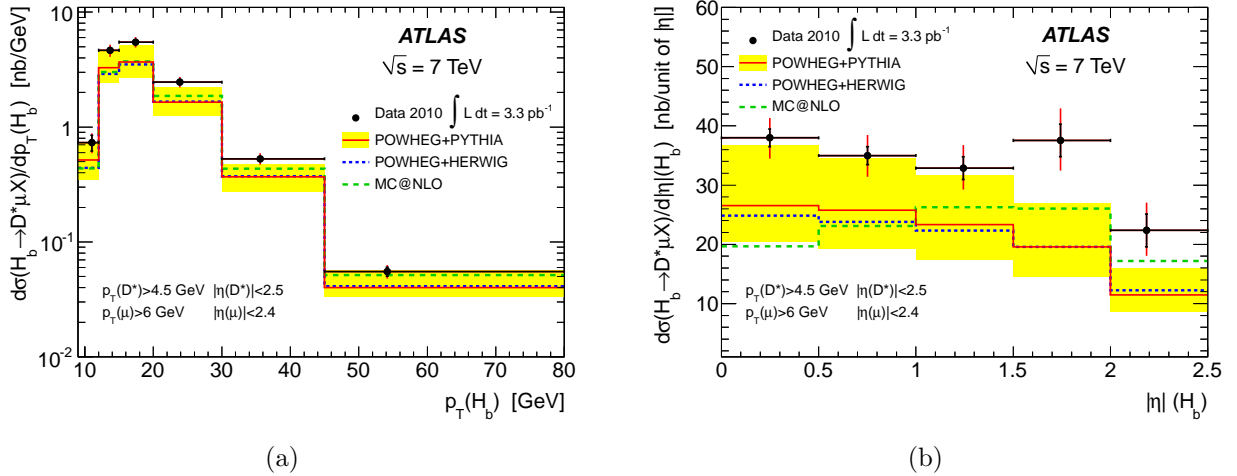


Figure 2: Differential cross section for $H_b \rightarrow D^{*+} \mu^- X$ production as a function of (a) p_T and (b) $|\eta|$ of the b -hadron, in the fiducial kinematical region $p_T(D^{*+}) > 4.5$ GeV, $p_T(\mu^-) > 6$ GeV, $|\eta(D^{*+})| < 2.5$ and $|\eta(\mu^-)| < 2.4$. The measurement is compared with the theoretical predictions, as described in the text. The inner error bars of the data points are statistical uncertainties, the outer are statistical+total systematic uncertainties.

10. Differential cross sections for b -hadron production

The b -hadron differential cross sections can be derived from the $H_b \rightarrow D^{*+} \mu^- X$ differential cross sections by taking into account the branching ratio $\mathcal{B}(b \rightarrow D^{*+} \mu^- X)$ and the necessary decay acceptance corrections. These are evaluated using a POWHEG+PYTHIA simulation in two steps:

- Identification of the H_b kinematic region selected by the D^{*+} and μ^- kinematic cuts. This indicates that only b -hadrons with $p_T(H_b) > 9$ GeV and $|\eta(H_b)| < 2.5$ pass the D^{*+} and μ^- kinematic cuts.
- Evaluation of a bin-by-bin p_T - and $|\eta|$ -decay acceptance α in the H_b allowed kinematic region, defined as

$$\alpha = \frac{\text{number of } H_b(\rightarrow D^{*+} \mu^-) \text{ passing the } D^* \text{ and } \mu \text{ kinematic cuts}}{\text{number of } H_b(\rightarrow D^{*+} \mu^-) \text{ passing the } H_b \text{ kinematic cuts}} \quad (11)$$

The results are shown in Table 9 for the POWHEG+PYTHIA central prediction. Section 8 describes how the NLO theoretical uncertainties are propagated to this measurement.

The b -hadron differential cross sections as a function of p_T and η , inside the kinematic region $p_T(H_b) > 9$ GeV and $|\eta(H_b)| < 2.5$, can then be calculated according to the formula:

$$\frac{d\sigma(H_b X)}{dp_T(\eta)} = \frac{1}{\alpha_{p_T(\eta)} \mathcal{B}(b \rightarrow D^{*+} \mu^- X)} \frac{d\sigma(pp \rightarrow H_b X' \rightarrow D^{*+} \mu^- X)}{dp_T(\eta)} \quad (12)$$

$p_T(H_b)$ [GeV]	$\frac{d\sigma(H_b \rightarrow D^{*+}\mu^- X)}{dp_T(H_b)}$ [nb/GeV]	$\frac{d\sigma(H_b X)}{dp_T(H_b)}$ [nb/GeV]
9–12	$0.73 \pm 0.12^{+0.09}_{-0.11}$	$(5.8 \pm 0.9^{+0.8}_{-1.0}) \cdot 10^3$
12–15	$4.65 \pm 0.27^{+0.50}_{-0.50}$	$(2.37 \pm 0.14^{+0.30}_{-0.33}) \cdot 10^3$
15–20	$5.48 \pm 0.19^{+0.57}_{-0.54}$	$(9.1 \pm 0.3^{+1.1}_{-1.1}) \cdot 10^2$
20–30	$2.46 \pm 0.08^{+0.26}_{-0.24}$	$212 \pm 7^{+26}_{-26}$
30–45	$0.530 \pm 0.025^{+0.056}_{-0.062}$	$31.3 \pm 1.5^{+3.9}_{-3.9}$
45–80	$0.055 \pm 0.005^{+0.007}_{-0.006}$	$2.78 \pm 0.25^{+0.38}_{-0.33}$

$ \eta(H_b) $	$\frac{d\sigma(H_b \rightarrow D^{*+}\mu^- X)}{d \eta(H_b) }$ [nb/unit of $ \eta $]	$\frac{d\sigma(H_b X)}{d \eta(H_b) }$ [μ b/unit of $ \eta $]
0.0–0.5	$38.0 \pm 1.5^{+3.3}_{-3.3}$	$14.3 \pm 0.6^{+1.7}_{-2.7}$
0.5–1.0	$35.0 \pm 1.5^{+3.2}_{-3.2}$	$13.4 \pm 0.6^{+1.8}_{-2.7}$
1.0–1.5	$32.9 \pm 1.9^{+3.3}_{-3.1}$	$13.1 \pm 0.7^{+2.1}_{-2.9}$
1.5–2.0	$37.5 \pm 2.7^{+4.7}_{-4.3}$	$15.8 \pm 1.1^{+2.4}_{-4.4}$
2.0–2.5	$22.3 \pm 2.8^{+3.8}_{-3.2}$	$13.3 \pm 1.6^{+2.5}_{-4.5}$

Table 6: Differential cross sections for $H_b \rightarrow D^{*+}\mu^- X$ and $H_b X$ production as a function of p_T and $|\eta|$ of the b -hadron, in the fiducial kinematical regions $p_T(D^{*+}) > 4.5$ GeV, $p_T(\mu^-) > 6$ GeV, $|\eta(D^{*+})| < 2.5$ and $|\eta(\mu^-)| < 2.4$, and $p_T(H_b) > 9$ GeV, $|\eta(H_b)| < 2.5$ respectively. The statistical and total systematic uncertainties are shown for each cross section.

Figure 3 shows the b -hadron differential cross section measurements compared with theoretical predictions. The shaded band is the overall theoretical uncertainty of the central POWHEG+PYTHIA prediction. Since the acceptance correction factors have a dependence on p_T and $|\eta|$, as shown in Table 9, the shapes of the b -hadron differential cross sections are different to the $H_b \rightarrow D^{*+}\mu^- X$ differential cross sections shown in Figure 2. The systematic uncertainties are those from the $\sigma(H_b \rightarrow D^{*+}\mu^- X)$ measurement described in Section 9, with the addition of the uncertainty of the branching ratio $\mathcal{B}(b \rightarrow D^{*+}\mu^- X)$ and the uncertainties of the decay acceptance correction. The b -hadron differential cross section values are reported in Table 6, together with the statistical and total systematic uncertainties, while the individual contributions to the systematic uncertainty are reported in Tables 7 and 8. The combined unfolding and acceptance uncertainties are calculated taking their correlations into account.

The comparison with data shows that NLO calculations underestimate the cross section, although the difference is within the combined experimental and theoretical uncertainties. The b -hadron integrated cross section for $p_T(H_b) > 9$ GeV and $|\eta(H_b)| < 2.5$ is measured as:

$$\sigma(pp \rightarrow H_b X) = 32.7 \pm 0.8 \text{ (stat.)} \pm 3.1 \text{ (syst.)}^{+2.1}_{-5.6}(\alpha) \pm 2.3(\mathcal{B}) \pm 1.1(\mathcal{L}) \mu\text{b}$$

The integrated POWHEG+PYTHIA prediction, with its theoretical uncertainty, is:

p_T bin (GeV)	9–12	12–15	15–20	20–30	30–45	45–80
data statistics	± 15.8	± 5.9	± 3.4	± 3.1	± 4.7	± 9.0
$\sigma(H_b \rightarrow D^{*+}\mu^-X)$ and $\sigma(H_b)$ relative systematic error (%)						
$D^*\mu$ fit	± 3.5	± 1.8	± 1.0	± 1.4	± 1.7	± 2.0
f_b	+2.5 -3.8	+2.3 -3.5	+1.8 -2.8	+1.6 -2.5	+1.4 -2.2	+1.8 -2.9
μ trigger	+1.3 -1.2	+1.3 -1.3	+1.7 -1.6	+2.2 -2.0	+2.5 -2.2	+2.7 -2.5
tracking + μ reconstruction	+9.1 -8.2	+9.0 -8.1	+8.9 -8.0	+8.7 -7.9	+8.5 -7.7	+8.3 -7.5
MC p_T/η reweight	+0.2 -1.3	+0.2 -1.2	+0.4 -1.1	+0.5 -1.1	+0.4 -1.0	+0.2 -0.8
D^0 and H_b vertices fit	± 2.0	± 2.0	± 2.0	± 2.0	± 2.0	± 2.0
D^0 mass correction	+0.8 -1.0	+0.8 -1.0	+0.8 -1.0	+0.8 -1.0	+0.8 -1.0	+0.8 -1.0
luminosity	± 3.4					
$\mathcal{B}(D^{*+} \rightarrow D^0\pi^+)$	± 0.7					
$\mathcal{B}(D^0 \rightarrow K^-\pi^+)$	± 1.3					
$\sigma(H_b \rightarrow D^{*+}\mu^-X)$ relative systematic error (%)						
unfolding	+6.6 -10.0	+2.3 -3.8	+1.7 -1.5	+2.3 -1.3	+3.2 -6.7	+9.1 -3.5
$\sigma(H_b)$ relative systematic error in (%)						
$\mathcal{B}(b \rightarrow D^{*+}\mu^-X)$	± 7					
unfolding \oplus acceptance	+3.4 -11.3	+1.6 -6.4	+2.3 -4.0	+0.7 -2.5	+1.7 -4.4	+6.0 -1.0
total syst $\sigma(H_b \rightarrow D^{*+}\mu^-X)$	+12.9 -14.7	+10.7 -10.8	+10.3 -9.9	+10.4 -9.8	+10.6 -11.7	+13.6 -10.3
total syst $\sigma(H_b)$	+13.4 -17.1	+12.6 -14.0	+12.5 -12.5	+12.3 -12.1	+12.3 -12.5	+13.5 -11.8

Table 7: $H_b \rightarrow D^{*+}\mu^-X$ and H_b cross section relative uncertainties as a function of $p_T(H_b)$, listed as percentages (%).

$$\sigma(pp \rightarrow H_b X) = 22.2_{-5.4}^{+8.9}(\text{scale})_{-1.9}^{+2.1}(m_b)_{-2.1}^{+2.2}(\text{PDF})_{-1.5}^{+1.6}(\text{hadr.}) \mu\text{b}$$

The corresponding POWHEG+HERWIG prediction is $18.6 \mu\text{b}$, while MC@NLO predicts $19.2 \mu\text{b}$, with similar theoretical uncertainties to the POWHEG+PYTHIA prediction.

11. Discussion

Section 10 discusses the measurement of the b -hadron production cross section for $p_T(H_b) > 9$ GeV and $|\eta(H_b)| < 2.5$. In order to compare this result with other LHC measurements, we extrapolate this measurement to the full kinematic phase space, extending to regions outside the ATLAS coverage, using the NLO MC theoretical predictions. The multiplicative extrapolation factor is defined as the ratio of the total number of generated b -hadrons to the number of b -hadrons generated with $p_T(H_b) > 9$ GeV and $|\eta(H_b)| < 2.5$, and is estimated to be $11.0_{-1.6}^{+2.6}$. The resulting total b -hadron cross section is:

$$\sigma(pp \rightarrow H_b X)_{\text{total}} = 360 \pm 9 (\text{stat.}) \pm 34 (\text{syst.}) \pm 25(\mathcal{B}) \pm 12(\mathcal{L})_{-69}^{+77}(\text{accept.} \oplus \text{extrap.}) \mu\text{b}$$

$ \eta $ bin	0–0.5	0.5–1	1–1.5	1.5–2	2–2.5	0–2.5
data statistics	± 3.9	± 4.3	± 5.8	± 7.3	± 12.5	± 2.5
$\sigma(H_b \rightarrow D^{*+} \mu^- X)$ and $\sigma(H_b)$ relative systematic error (%)						
$D^* \mu$ fit	± 0.7	± 0.9	± 0.7	± 1.2	± 1.0	± 0.5
f_b	+1.6 -2.6	+2.0 -3.5	+1.5 -2.4	+1.5 -2.6	+1.3 -2.1	+1.7 -2.8
μ trigger	+2.0 -1.9	+2.1 -1.9	+1.8 -1.6	+1.7 -1.6	+1.6 -1.5	+1.9 -1.9
tracking + μ reconstruction	+7.0 -6.5	+7.1 -6.6	+8.5 -7.7	+11.4 -10.0	+16.2 -13.4	+8.6 -8.0
MC p_T/η reweight	+1.5 -0.1	+1.2 -0.1	+1.4 -0.1	+1.1 -0.2	+2.0 -0.5	+1.3 -1.3
D^0 and H_b vertices fit	± 2.0	± 2.0	± 2.0	± 2.0	± 2.0	± 2.0
D^0 mass correction	+0.8 -1.0	+0.8 -1.0	+0.8 -1.0	+0.8 -1.0	+0.8 -1.0	+0.8 -1.0
luminosity	± 3.4					
$\mathcal{B}(D^{*+} \rightarrow D^0 \pi^+)$	± 0.7					
$\mathcal{B}(D^0 \rightarrow K^- \pi^+)$	± 1.3					
$\sigma(H_b \rightarrow D^{*+} \mu^- X)$ relative systematic error (%)						
unfolding	+1.3 -0.9	+1.1 -1.5	+1.4 -0.8	+0.7 -1.0	+1.1 -2.0	-
$\sigma(H_b)$ relative systematic error (%)						
$\mathcal{B}(b \rightarrow D^{*+} \mu^- X)$	± 7					
unfolding \oplus acceptance	+5.1 -15.0	+7.3 -16.2	+10.7 -19.1	+4.8 -24.6	+4.3 -29.6	+6.4 -17.1
total syst $\sigma(H_b \rightarrow D^{*+} \mu^- X)$	+8.8 -8.5	+9.0 -9.0	+10.0 -9.4	+12.5 -11.4	+17.1 -14.5	+10.0 -9.8
total syst $\sigma(H_b)$	+12.2 -18.5	+13.4 -19.7	+16.1 -22.3	+15.0 -27.9	+18.8 -33.5	+13.8 -20.9

Table 8: $H_b \rightarrow D^{*+} \mu^- X$ and H_b cross section relative uncertainties as a function of $|\eta(H_b)|$, listed as percentages (%). The last column refers to the integrated cross sections.

where the combined acceptance and extrapolation uncertainty is calculated taking their correlations into account.

This value can be compared with the inclusive $b\bar{b}$ cross section measurements by LHCb $\sigma(pp \rightarrow b\bar{b}X) = 284 \pm 20$ (stat.) ± 49 (syst.) μb , evaluated in the kinematic region $2 < \eta < 6$ using decays to $D^0 \mu^- \bar{\nu} X$ final states [16], and $\sigma(pp \rightarrow b\bar{b}X) = 288 \pm 4$ (stat.) ± 48 (syst.) μb , evaluated using $J/\psi X$ final states in the kinematic region $2.0 < y < 4.5$ [17]. Extrapolations outside the LHCb sensitivity region are done using different theoretical models, without including additional uncertainties. Also ALICE measured the inclusive $b\bar{b}$ cross section in pp collisions, using decays to $J/\psi X$ final states in the kinematic region $|y| < 0.9$ and $p_T > 1.3$ GeV [24]. After extrapolation to the full phase space, they obtain $\sigma(pp \rightarrow b\bar{b}X) = 244 \pm 64$ (stat.) $^{+50}_{-59}$ (syst.) $^{+7}_{-6}$ (extr.) μb .

$p_T(H_b)$	α
9–12 GeV	0.005
12–15 GeV	0.071
15–20 GeV	0.219
20–30 GeV	0.422
30–45 GeV	0.614
45–80 GeV	0.723

$ \eta(H_b) $	α
0.0–0.5	0.096
0.5–1.0	0.095
1.0–1.5	0.091
1.5–2.0	0.086
2.0–2.5	0.061

Table 9: Decay acceptance α as a function of $p_T(H_b)$ and $|\eta(H_b)|$ for the POWHEG+PYTHIA prediction.

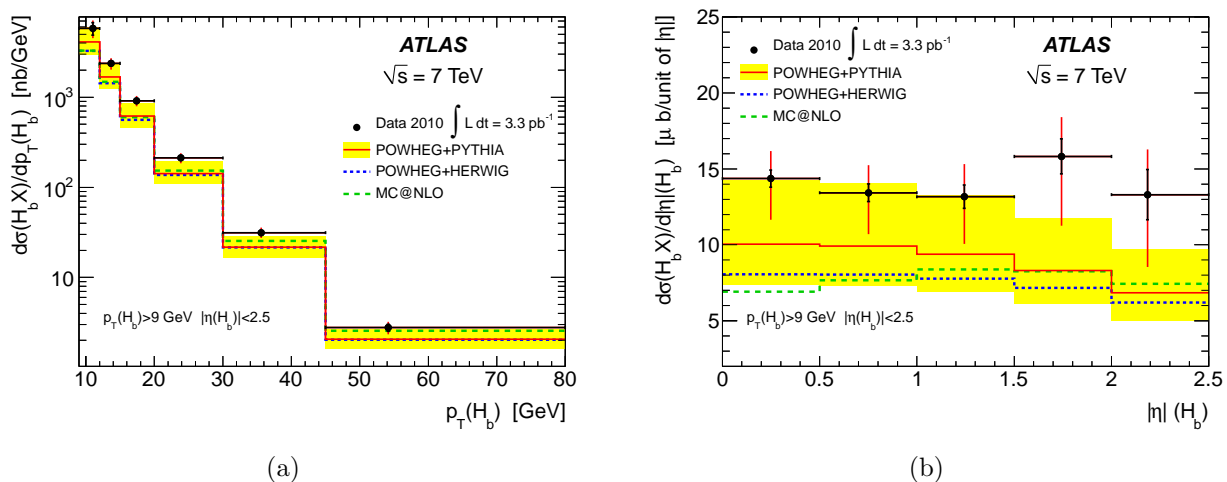


Figure 3: Differential cross section for H_b production as a function of (a) p_T and (b) $|\eta|$ of the b -hadron, in the fiducial kinematical region $p_T(H_b) > 9$ GeV, $|\eta(H_b)| < 2.5$. The measurement is compared with the theoretical predictions, as described in the text. The inner error bars of the data points are statistical uncertainties, the outer are statistical+total systematic uncertainties.

12. Conclusions

The production of b -hadrons (H_b) at the LHC is measured with the ATLAS detector in proton-proton collisions at $\sqrt{s} = 7$ TeV, using 3.3 pb^{-1} of integrated luminosity from the 2010 run. A b -hadron enriched sample was obtained by combining oppositely charged D^* mesons and muons, in events triggered by a muon with p_T exceeding 6 GeV.

Differential cross sections as functions of p_T and $|\eta|$ are produced for both H_b and $H_b \rightarrow D^{*+} \mu^- X$ production. These measurements are found to be higher than the NLO QCD predictions, but consistent within the experimental and theoretical uncertainties. The integrated b -hadron cross section for $p_T(H_b) > 9$ GeV and $|\eta(H_b)| < 2.5$ is measured as

$$\sigma(pp \rightarrow H_b X) = 32.7 \pm 0.8 \text{ (stat.)} \pm 3.1 \text{ (syst.)}_{-5.6}^{+2.1}(\alpha) \pm 2.3(\mathcal{B}) \pm 1.1(\mathcal{L}) \mu\text{b}.$$

13. Acknowledgements

We thank CERN for the very successful operation of the LHC, as well as the support staff from our institutions without whom ATLAS could not be operated efficiently.

We acknowledge the support of ANPCyT, Argentina; YerPhI, Armenia; ARC, Australia; BMWF, Austria; ANAS, Azerbaijan; SSTC, Belarus; CNPq and FAPESP, Brazil; NSERC, NRC and CFI, Canada; CERN; CONICYT, Chile; CAS, MOST and NSFC, China; COLCIENCIAS, Colombia; MSMT CR, MPO CR and VSC CR, Czech Republic; D NRF, DNSRC and Lundbeck Foundation, Denmark; EPLANET and ERC, European Union; IN2P3-CNRS, CEA-DSM/IRFU, France; GNAS, Georgia; BMBF, DFG, HGF, MPG and AvH Foundation, Germany; GSRT, Greece; ISF, MINERVA, GIF, DIP and Benoziyo Center, Israel; INFN, Italy; MEXT and JSPS, Japan; CNRST, Morocco; FOM and NWO, Netherlands; RCN, Norway; MNiSW, Poland; GRICES and FCT, Portugal; MERYS (MECTS), Romania; MES of Russia and ROSATOM, Russian Federation; JINR; MSTD, Serbia; MSSR, Slovakia; ARRS and MVZT, Slovenia; DST/NRF, South Africa; MICINN, Spain; SRC and Wallenberg Foundation, Sweden; SER, SNSF and Cantons of Bern and Geneva, Switzerland; NSC, Taiwan; TAEK, Turkey; STFC, the Royal Society and Leverhulme Trust, United Kingdom; DOE and NSF, United States of America.

The crucial computing support from all WLCG partners is acknowledged gratefully, in particular from CERN and the ATLAS Tier-1 facilities at TRIUMF (Canada), NDGF (Denmark, Norway, Sweden), CC-IN2P3 (France), KIT/GridKA (Germany), INFN-CNAF (Italy), NL-T1 (Netherlands), PIC (Spain), ASGC (Taiwan), RAL (UK) and BNL (USA) and in the Tier-2 facilities worldwide.

References

- [1] P. Nason, S. Dawson and R.K. Ellis, “The total cross section for the production of heavy quarks in hadronic collisions”, Nucl. Phys. B 303 (1988) 607.
- [2] P. Nason, S. Dawson and R.K. Ellis, “The one particle inclusive differential cross section for heavy quark production in hadronic collisions”, Nucl. Phys. B 327 (1989) 49.
- [3] UA1 Collaboration, “Beauty Production at the CERN Proton- anti-Proton Collider”, Phys. Lett. B 186 (1987) 237.
- [4] UA1 Collaboration, “Measurement of the Bottom Quark Production Cross Section in Proton-anti-Proton Collisions at $\sqrt{s} = 0.63$ TeV”, Phys. Lett. B 213 (1988) 405.
- [5] CDF Collaboration, “Measurement of the Ratio of the b Quark Production Cross Sections in $p\bar{p}$ Collisions at $\sqrt{s} = 630$ GeV and $\sqrt{s} = 1800$ GeV”, Phys. Rev. D 66 (2002) 032002.
- [6] CDF Collaboration, “Measurement of the bottom quark production cross-section using semileptonic decay electron in $p\bar{p}$ collisions at $\sqrt{s} = 1.8$ TeV”, Phys. Rev. Lett. 71 (1993) 500.
- [7] CDF Collaboration, “Measurement of the B meson differential cross-section, $d\sigma/dp_T$, in $p\bar{p}$ collisions at $\sqrt{s} = 1.8$ TeV”, Phys. Rev. Lett. 75 (1995) 1451.
- [8] CDF Collaboration, “Measurement of the B^+ total cross section and B^+ differential cross section $d\sigma/dp_T$ in $p\bar{p}$ collisions at $\sqrt{s} = 1.8$ TeV”, Phys. Rev. D 65 (2002) 052005.
- [9] D0 Collaboration, “Inclusive μ and B quark production cross-sections in $p\bar{p}$ collisions at $\sqrt{s} = 1.8$ TeV”, Phys. Rev. Lett. 74 (1995) 3548.
- [10] D0 Collaboration, “Small angle muon and bottom quark production in $p\bar{p}$ collisions at $\sqrt{s} = 1.8$ TeV”, Phys. Rev. Lett. 84 (2000) 5478.

- [11] D0 Collaboration, “Cross section for b jet production in $p\bar{p}$ collisions at $\sqrt{s} = 1.8$ TeV”, Phys. Rev. Lett. 85 (2000) 5068.
- [12] CDF Collaboration, “Measurement of the J/ψ meson and b -hadron production cross sections in $p\bar{p}$ collisions at $\sqrt{s} = 1960$ GeV”, Phys. Rev. D 71 (2005) 032001.
- [13] CDF Collaboration, “Measurement of the B^+ production cross section in $p\bar{p}$ collisions at $\sqrt{s} = 1960$ GeV”, Phys. Rev. D 75 (2007) 012010.
- [14] CDF Collaboration, “Measurement of the b -hadron production cross section using decays to $\mu^- D^0 X$ final states in $p\bar{p}$ collisions at $\sqrt{s} = 1960$ GeV”, Phys. Rev. D 79 (2009) 092003.
- [15] M. Cacciari, S. Frixione, M. Mangano et al., “QCD analysis of first b cross-section data at 1.96TeV”, JHEP 0407 (2004) 033.
- [16] LHCb Collaboration, “Measurement of $\sigma(b\bar{b})$ at $\sqrt{s} = 7$ TeV in the forward region”, Phys. Lett. B 694 (2010) 209.
- [17] LHCb Collaboration, “Measurement of J/ψ production in pp collisions at $\sqrt{s} = 7$ TeV”, Eur. Phys. J. C 71 (2011) 1645.
- [18] LHCb Collaboration, “Measurement of the B^\pm production cross-section in pp collisions at $\sqrt{s} = 7$ TeV”, arXiv:1202.4812.
- [19] CMS Collaboration, “Measurement of the B^+ Production Cross Section in pp Collisions at $\sqrt{s} = 7$ TeV”, Phys. Rev. Lett. 106 (2011) 112001.
- [20] CMS Collaboration, “Measurement of the B^0 Production Cross Section in pp Collisions at $\sqrt{s} = 7$ TeV”, Phys. Rev. Lett. 106 (2011) 252001.
- [21] CMS Collaboration, “Measurement of the B_s^0 Production Cross Section with $B_s^0 \rightarrow J/\psi\phi$ Decays in pp Collisions at $\sqrt{s} = 7$ TeV”, Phys. Rev. D 84 (2011) 052008.
- [22] CMS Collaboration, “Inclusive b -hadron production cross section with muons in pp collisions at $\sqrt{s} = 7$ TeV”, JHEP 03 (2011) 090.
- [23] CMS Collaboration, “Measurement of the cross section for production of $b\bar{b}X$, decaying to muons in pp collisions at $\sqrt{s} = 7$ TeV”, arXiv:1203.3458.
- [24] ALICE Collaboration, “Measurement of prompt and non-prompt J/ψ production cross sections at mid-rapidity in pp collisions at $\sqrt{s} = 7$ TeV”, arXiv:1205.5880v1.
- [25] ATLAS Collaboration, “The ATLAS Experiment at the CERN Large Hadron Collider”, JINST 3 S08003 (2008).
- [26] K. Nakamura et al. (Particle Data Group), J. Phys. G 37, 075021 (2010).
- [27] T. Sjostrand, S. Mrenna, P. Skands, “PYTHIA 6.4 Physics and Manual”, JHEP 05 (2006) 026.
- [28] ATLAS Collaboration, “Charged-particle multiplicities in pp interactions measured with the ATLAS detector at the LHC”, New J. Phys. 13 (2011) 053033.
- [29] ATLAS Collaboration, “The ATLAS Simulation Infrastructure”, Eur. Phys. J. C 70 (2010) 823.
- [30] S. Agostinelli et al., “GEANT4: A simulation toolkit”, Nucl. Instrum. Meth. A 506 (2003) 250.
- [31] S. Frixione and B. R. Webber, “Matching NLO QCD computations and parton shower simulations”, JHEP 0206 (2002) 029.
- [32] S. Frixione, P. Nason and B. R. Webber, “Matching NLO QCD and parton showers in heavy flavour production”, JHEP 0308 (2003) 007.
- [33] P. Nason, “A new method for combining NLO QCD with shower Monte Carlo algorithms”, JHEP 0411 (2004) 040.
- [34] S. Frixione, P. Nason and G. Ridolfi, “A Positive-Weight Next-to-Leading-Order Monte Carlo for Heavy Flavour Hadroproduction”, JHEP 0709 (2007) 126.
- [35] G. Corcella et al. , “HERWIG 6: an event generator for Hadron Emission Reactions With Interfering Gluons”, JHEP 0101 (2001) 010.
- [36] P. M. Nadolsky, “Implications of CTEQ global analysis for collider observables”, Phys. Rev. D 78 (2008) 013004.
- [37] B. R. Webber, “A QCD model for jet fragmentation including soft gluon interference”, Nucl. Phys. B 238 (1984) 492.
- [38] B. Anderson et al., “Parton fragmentation and string dynamics”, Phys. Rep. 97 (1983) 31.

- [39] M. G. Bowler, “ e^+e^- Production of Heavy Quarks in the String Model”, *Z. Phys. C* 11 (1981) 169.
- [40] B. Anderson, G. Gustafson, B. Soederberg, “A General Model for Jet Fragmentation”, *Z. Phys. C* 20 (1983) 317.
- [41] C. Peterson et al., “Scaling violations in Inclusive e^+e^- Annihilation Spectra”, *Phys. Rev. D* 27 (1983) 105.
- [42] ATLAS Collaboration, “Measurement of the differential cross-sections of inclusive, prompt and non-prompt J/ψ production in proton-proton collisions at $\sqrt{s} = 7$ TeV”, *Nucl. Phys. B* 850 (2011) 387.
- [43] ATLAS Collaboration, “Luminosity Determination in pp Collisions at $\sqrt{s} = 7$ TeV Using the ATLAS Detector at the LHC”, *Eur. Phys. J. C* 71 (2011) 1630.
- [44] ATLAS Collaboration, “Updated Luminosity Determination in pp Collisions at $\sqrt{s} = 7$ TeV using the ATLAS Detector”, ATLAS-CONF-2011-011, 2011.
- [45] G. Cowan, “A Survey of Unfolding Methods for Particle Physics”, *Proc. Advanced Statistical Techniques in Particle Physics, Durham (2002)*.
- [46] G. Cowan, “Statistical Data Analysis”, Oxford University Press (1998).
- [47] V. Blobel, “Unfolding Methods in High Energy Physics”, DESY 84-118 (1982), CERN 85-02 (1985).
- [48] G. Zech, “Comparing statistical data to Monte Carlo simulation - parameter fitting and unfolding”, DESY 95-113 (1995).
- [49] G. D’Agostini, “A Multidimensional unfolding method based on Bayes’ theorem”, *Nucl. Instrum. Meth. A* 362 (1995) 487.

The ATLAS Collaboration

G. Aad⁴⁸, B. Abbott¹¹¹, J. Abdallah¹¹, S. Abdel Khalek¹¹⁵, A.A. Abdelalim⁴⁹, O. Abdinov¹⁰, B. Abi¹¹², M. Abolins⁸⁸, O.S. AbouZeid¹⁵⁸, H. Abramowicz¹⁵³, H. Abreu¹³⁶, E. Acerbi^{89a,89b}, B.S. Acharya^{164a,164b}, L. Adamczyk³⁷, D.L. Adams²⁴, T.N. Addy⁵⁶, J. Adelman¹⁷⁶, S. Adomeit⁹⁸, P. Adragna⁷⁵, T. Adye¹²⁹, S. Aefsky²², J.A. Aguilar-Saavedra^{124b,a}, M. Agustoni¹⁶, M. Aharrouche⁸¹, S.P. Ahlen²¹, F. Ahles⁴⁸, A. Ahmad¹⁴⁸, M. Ahsan⁴⁰, G. Aielli^{133a,133b}, T. Akdogan^{18a}, T.P.A. Åkesson⁷⁹, G. Akimoto¹⁵⁵, A.V. Akimov⁹⁴, M.S. Alam¹, M.A. Alam⁷⁶, J. Albert¹⁶⁹, S. Albrand⁵⁵, M. Aleksa²⁹, I.N. Aleksandrov⁶⁴, F. Alessandria^{89a}, C. Alexa^{25a}, G. Alexander¹⁵³, G. Alexandre⁴⁹, T. Alexopoulos⁹, M. Alhroob^{164a,164c}, M. Aliev¹⁵, G. Alimonti^{89a}, J. Alison¹²⁰, B.M.M. Allbrooke¹⁷, P.P. Allport⁷³, S.E. Allwood-Spiers⁵³, J. Almond⁸², A. Aloisio^{102a,102b}, R. Alon¹⁷², A. Alonso⁷⁹, B. Alvarez Gonzalez⁸⁸, M.G. Alviggi^{102a,102b}, K. Amako⁶⁵, C. Amelung²², V.V. Ammosov¹²⁸, A. Amorim^{124a,b}, N. Amram¹⁵³, C. Anastopoulos²⁹, L.S. Ancu¹⁶, N. Andari¹¹⁵, T. Andeen³⁴, C.F. Anders^{58b}, G. Anders^{58a}, K.J. Anderson³⁰, A. Andreazza^{89a,89b}, V. Andrei^{58a}, X.S. Anduaga⁷⁰, P. Anger⁴³, A. Angerami³⁴, F. Anghinolfi²⁹, A. Anisenkov¹⁰⁷, N. Anjos^{124a}, A. Annovi⁴⁷, A. Antonaki⁸, M. Antonelli⁴⁷, A. Antonov⁹⁶, J. Antos^{144b}, F. Anulli^{132a}, S. Aoun⁸³, L. Aperio Bella⁴, R. Apolle^{118,c}, G. Arabidze⁸⁸, I. Aracena¹⁴³, Y. Arai⁶⁵, A.T.H. Arce⁴⁴, S. Arfaoui¹⁴⁸, J-F. Arguin¹⁴, E. Arik^{18a,*}, M. Arik^{18a}, A.J. Armbruster⁸⁷, O. Arnaez⁸¹, V. Arnal⁸⁰, C. Arnault¹¹⁵, A. Artamonov⁹⁵, G. Artoni^{132a,132b}, D. Arutinov²⁰, S. Asai¹⁵⁵, R. Asfandiyarov¹⁷³, S. Ask²⁷, B. Åsman^{146a,146b}, L. Asquith⁵, K. Assamagan²⁴, A. Astbury¹⁶⁹, B. Aubert⁴, E. Auge¹¹⁵, K. Augsten¹²⁷, M. Auresseau^{145a}, G. Avolio¹⁶³, R. Avramidou⁹, D. Axen¹⁶⁸, G. Azuelos^{93,d}, Y. Azuma¹⁵⁵, M.A. Baak²⁹, G. Baccaglioni^{89a}, C. Bacci^{134a,134b}, A.M. Bach¹⁴, H. Bachacou¹³⁶, K. Bachas²⁹, M. Backes⁴⁹, M. Backhaus²⁰, E. Badescu^{25a}, P. Bagnaia^{132a,132b}, S. Bahinipati², Y. Bai^{32a}, D.C. Bailey¹⁵⁸, T. Bain¹⁵⁸, J.T. Baines¹²⁹, O.K. Baker¹⁷⁶, M.D. Baker²⁴, S. Baker⁷⁷, E. Banas³⁸, P. Banerjee⁹³, Sw. Banerjee¹⁷³, D. Banfi²⁹, A. Bangert¹⁵⁰, V. Bansal¹⁶⁹, H.S. Bansil¹⁷, L. Barak¹⁷², S.P. Baranov⁹⁴, A. Barbaro Galtieri¹⁴, T. Barber⁴⁸, E.L. Barberio⁸⁶, D. Barberis^{50a,50b}, M. Barbero²⁰, D.Y. Bardin⁶⁴, T. Barillari⁹⁹, M. Barisonzi¹⁷⁵, T. Barklow¹⁴³, N. Barlow²⁷, B.M. Barnett¹²⁹, R.M. Barnett¹⁴, A. Baroncelli^{134a}, G. Barone⁴⁹, A.J. Barr¹¹⁸, F. Barreiro⁸⁰, J. Barreiro Guimarães da Costa⁵⁷, P. Barrillon¹¹⁵, R. Bartoldus¹⁴³, A.E. Barton⁷¹, V. Bartsch¹⁴⁹, R.L. Bates⁵³, L. Batkova^{144a}, J.R. Batley²⁷, A. Battaglia¹⁶, M. Battistin²⁹, F. Bauer¹³⁶, H.S. Bawa^{143,e}, S. Beale⁹⁸, T. Beau⁷⁸, P.H. Beauchemin¹⁶¹, R. Beccherle^{50a}, P. Bechtel²⁰, H.P. Beck¹⁶, A.K. Becker¹⁷⁵, S. Becker⁹⁸, M. Beckingham¹³⁸, K.H. Becks¹⁷⁵, A.J. Beddall^{18c}, A. Beddall^{18c}, S. Bedikian¹⁷⁶, V.A. Bednyakov⁶⁴, C.P. Bee⁸³, M. Begel²⁴, S. Behar Harpaz¹⁵², M. Beimforde⁹⁹, C. Belanger-Champagne⁸⁵, P.J. Bell⁴⁹, W.H. Bell⁴⁹, G. Bella¹⁵³, L. Bellagamba^{19a}, F. Bellina²⁹, M. Bellomo²⁹, A. Belloni⁵⁷, O. Beloborodova^{107,f}, K. Belotskiy⁹⁶, O. Beltramello²⁹, O. Benary¹⁵³, D. Bencheikroun^{135a}, K. Bendtz^{146a,146b}, N. Benekos¹⁶⁵, Y. Benhammou¹⁵³, E. Benhar Nocchioli⁴⁹, J.A. Benitez Garcia^{159b}, D.P. Benjamin⁴⁴, M. Benoit¹¹⁵, J.R. Bensinger²², K. Benslama¹³⁰, S. Bentvelsen¹⁰⁵, D. Berge²⁹, E. Bergeaas Kuutmann⁴¹, N. Berger⁴, F. Berghaus¹⁶⁹, E. Berglund¹⁰⁵, J. Beringer¹⁴, P. Bernat⁷⁷, R. Bernhard⁴⁸,

C. Bernius²⁴, T. Berry⁷⁶, C. Bertella⁸³, A. Bertin^{19a,19b}, F. Bertolucci^{122a,122b},
 M.I. Besana^{89a,89b}, G.J. Besjes¹⁰⁴, N. Besson¹³⁶, S. Bethke⁹⁹, W. Bhimji⁴⁵, R.M. Bianchi²⁹,
 M. Bianco^{72a,72b}, O. Biebel⁹⁸, S.P. Bieniek⁷⁷, K. Bierwagen⁵⁴, J. Biesiada¹⁴, M. Biglietti^{134a},
 H. Bilokon⁴⁷, M. Bindi^{19a,19b}, S. Binet¹¹⁵, A. Bingul^{18c}, C. Bini^{132a,132b}, C. Biscarat¹⁷⁸,
 U. Bitenc⁴⁸, K.M. Black²¹, R.E. Blair⁵, J.-B. Blanchard¹³⁶, G. Blanchot²⁹, T. Blazek^{144a},
 C. Blocker²², J. Blocki³⁸, A. Blondel⁴⁹, W. Blum⁸¹, U. Blumenschein⁵⁴, G.J. Bobbink¹⁰⁵,
 V.B. Bobrovnikov¹⁰⁷, S.S. Bocchetta⁷⁹, A. Bocci⁴⁴, C.R. Boddy¹¹⁸, M. Boehler⁴¹,
 J. Boek¹⁷⁵, N. Boelaert³⁵, J.A. Bogaerts²⁹, A. Bogdanchikov¹⁰⁷, A. Bogouch^{90,*},
 C. Boehm^{146a}, J. Boehm¹²⁵, V. Boisvert⁷⁶, T. Bold³⁷, V. Boldea^{25a}, N.M. Bolnet¹³⁶,
 M. Bomben⁷⁸, M. Bona⁷⁵, M. Boonekamp¹³⁶, C.N. Booth¹³⁹, S. Bordoni⁷⁸, C. Borer¹⁶,
 A. Borisov¹²⁸, G. Borissov⁷¹, I. Borjanovic^{12a}, M. Borri⁸², S. Borroni⁸⁷,
 V. Bortolotto^{134a,134b}, K. Bos¹⁰⁵, D. Boscherini^{19a}, M. Bosman¹¹, H. Boterenbrood¹⁰⁵,
 D. Botterill¹²⁹, J. Bouchami⁹³, J. Boudreau¹²³, E.V. Bouhova-Thacker⁷¹, D. Boumediene³³,
 C. Bourdarios¹¹⁵, N. Bousson⁸³, A. Boveia³⁰, J. Boyd²⁹, I.R. Boyko⁶⁴,
 I. Bozovic-Jelisavcic^{12b}, J. Bracinik¹⁷, P. Branchini^{134a}, A. Brandt⁷, G. Brandt¹¹⁸,
 O. Brandt⁵⁴, U. Bratzler¹⁵⁶, B. Brau⁸⁴, J.E. Brau¹¹⁴, H.M. Braun¹⁷⁵, S.F. Brazzale^{164a,164c},
 B. Brelier¹⁵⁸, J. Bremer²⁹, K. Brendlinger¹²⁰, R. Brenner¹⁶⁶, S. Bressler¹⁷², D. Britton⁵³,
 F.M. Brochu²⁷, I. Brock²⁰, R. Brock⁸⁸, E. Brodet¹⁵³, F. Broggi^{89a}, C. Bromberg⁸⁸,
 J. Bronner⁹⁹, G. Brooijmans³⁴, T. Brooks⁷⁶, W.K. Brooks^{31b}, G. Brown⁸², H. Brown⁷,
 P.A. Bruckman de Renstrom³⁸, D. Bruncko^{144b}, R. Bruneliere⁴⁸, S. Brunet⁶⁰, A. Bruni^{19a},
 G. Bruni^{19a}, M. Bruschi^{19a}, T. Buanes¹³, Q. Buat⁵⁵, F. Bucci⁴⁹, J. Buchanan¹¹⁸,
 P. Buchholz¹⁴¹, R.M. Buckingham¹¹⁸, A.G. Buckley⁴⁵, S.I. Buda^{25a}, I.A. Budagov⁶⁴,
 B. Budick¹⁰⁸, V. Büscher⁸¹, L. Bugge¹¹⁷, O. Bulekov⁹⁶, A.C. Bundock⁷³, M. Bunse⁴²,
 T. Buran¹¹⁷, H. Burckhart²⁹, S. Burdin⁷³, T. Burgess¹³, S. Burke¹²⁹, E. Busato³³,
 P. Bussey⁵³, C.P. Buszello¹⁶⁶, B. Butler¹⁴³, J.M. Butler²¹, C.M. Buttar⁵³,
 J.M. Butterworth⁷⁷, W. Buttinger²⁷, S. Cabrera Urbán¹⁶⁷, D. Caforio^{19a,19b}, O. Cakir^{3a},
 P. Calafiura¹⁴, G. Calderini⁷⁸, P. Calfayan⁹⁸, R. Calkins¹⁰⁶, L.P. Caloba^{23a},
 R. Caloi^{132a,132b}, D. Calvet³³, S. Calvet³³, R. Camacho Toro³³, P. Camarri^{133a,133b},
 D. Cameron¹¹⁷, L.M. Caminada¹⁴, S. Campana²⁹, M. Campanelli⁷⁷, V. Canale^{102a,102b},
 F. Canelli^{30,g}, A. Canepa^{159a}, J. Cantero⁸⁰, R. Cantrill⁷⁶, L. Capasso^{102a,102b},
 M.D.M. Capeans Garrido²⁹, I. Caprini^{25a}, M. Caprini^{25a}, D. Capriotti⁹⁹, M. Capua^{36a,36b},
 R. Caputo⁸¹, R. Cardarelli^{133a}, T. Carli²⁹, G. Carlino^{102a}, L. Carminati^{89a,89b}, B. Caron⁸⁵,
 S. Caron¹⁰⁴, E. Carquin^{31b}, G.D. Carrillo Montoya¹⁷³, A.A. Carter⁷⁵, J.R. Carter²⁷,
 J. Carvalho^{124a,h}, D. Casadei¹⁰⁸, M.P. Casado¹¹, M. Cascella^{122a,122b}, C. Caso^{50a,50b,*},
 A.M. Castaneda Hernandez^{173,i}, E. Castaneda-Miranda¹⁷³, V. Castillo Gimenez¹⁶⁷,
 N.F. Castro^{124a}, G. Cataldi^{72a}, P. Catastini⁵⁷, A. Catinaccio²⁹, J.R. Catmore²⁹, A. Cattai²⁹,
 G. Cattani^{133a,133b}, S. Caughron⁸⁸, P. Cavalleri⁷⁸, D. Cavalli^{89a}, M. Cavalli-Sforza¹¹,
 V. Cavasinni^{122a,122b}, F. Ceradini^{134a,134b}, A.S. Cerqueira^{23b}, A. Cerri²⁹, L. Cerrito⁷⁵,
 F. Cerutti⁴⁷, S.A. Cetin^{18b}, A. Chafaq^{135a}, D. Chakraborty¹⁰⁶, I. Chalupkova¹²⁶, K. Chan²,
 B. Chapleau⁸⁵, J.D. Chapman²⁷, J.W. Chapman⁸⁷, E. Chareyre⁷⁸, D.G. Charlton¹⁷,
 V. Chavda⁸², C.A. Chavez Barajas²⁹, S. Cheatham⁸⁵, S. Chekanov⁵, S.V. Chekulaev^{159a},
 G.A. Chelkov⁶⁴, M.A. Chelstowska¹⁰⁴, C. Chen⁶³, H. Chen²⁴, S. Chen^{32c}, X. Chen¹⁷³,
 Y. Chen³⁴, A. Cheplakov⁶⁴, R. Cherkaoui El Moursli^{135e}, V. Chernyatin²⁴, E. Cheu⁶,

S.L. Cheung¹⁵⁸, L. Chevalier¹³⁶, G. Chiefari^{102a,102b}, L. Chikovani^{51a}, J.T. Childers²⁹,
 A. Chilingarov⁷¹, G. Chiodini^{72a}, A.S. Chisholm¹⁷, R.T. Chislett⁷⁷, A. Chitan^{25a},
 M.V. Chizhov⁶⁴, G. Choudalakis³⁰, S. Chouridou¹³⁷, I.A. Christidi⁷⁷, A. Christov⁴⁸,
 D. Chromek-Burckhart²⁹, M.L. Chu¹⁵¹, J. Chudoba¹²⁵, G. Ciapetti^{132a,132b}, A.K. Ciftci^{3a},
 R. Ciftci^{3a}, D. Cinca³³, V. Cindro⁷⁴, C. Ciocca^{19a,19b}, A. Ciocio¹⁴, M. Cirilli⁸⁷,
 P. Cirkovic^{12b}, M. Citterio^{89a}, M. Ciubancan^{25a}, A. Clark⁴⁹, P.J. Clark⁴⁵, R.N. Clarke¹⁴,
 W. Cleland¹²³, J.C. Clemens⁸³, B. Clement⁵⁵, C. Clement^{146a,146b}, Y. Coadou⁸³,
 M. Cobal^{164a,164c}, A. Coccaro¹³⁸, J. Cochran⁶³, J.G. Cogan¹⁴³, J. Coggeshall¹⁶⁵,
 E. Cogneras¹⁷⁸, J. Colas⁴, A.P. Colijn¹⁰⁵, N.J. Collins¹⁷, C. Collins-Tooth⁵³, J. Collot⁵⁵,
 T. Colombo^{119a,119b}, G. Colon⁸⁴, P. Conde Muiño^{124a}, E. Coniavitis¹¹⁸, M.C. Conidi¹¹,
 S.M. Consonni^{89a,89b}, V. Consorti⁴⁸, S. Constantinescu^{25a}, C. Conta^{119a,119b}, G. Conti⁵⁷,
 F. Conventi^{102a,j}, M. Cooke¹⁴, B.D. Cooper⁷⁷, A.M. Cooper-Sarkar¹¹⁸, K. Copic¹⁴,
 T. Cornelissen¹⁷⁵, M. Corradi^{19a}, F. Corriveau^{85,k}, A. Cortes-Gonzalez¹⁶⁵, G. Cortiana⁹⁹,
 G. Costa^{89a}, M.J. Costa¹⁶⁷, D. Costanzo¹³⁹, T. Costin³⁰, D. Côte²⁹, L. Courneyea¹⁶⁹,
 G. Cowan⁷⁶, C. Cowden²⁷, B.E. Cox⁸², K. Cranmer¹⁰⁸, F. Crescioli^{122a,122b},
 M. Cristinziani²⁰, G. Crosetti^{36a,36b}, R. Crupi^{72a,72b}, S. Crépe-Renaudin⁵⁵, C.-M. Cuciuc^{25a},
 C. Cuenca Almenar¹⁷⁶, T. Cuhadar Donszelmann¹³⁹, M. Curatolo⁴⁷, C.J. Curtis¹⁷,
 C. Cuthbert¹⁵⁰, P. Cwetanski⁶⁰, H. Czirr¹⁴¹, P. Czodrowski⁴³, Z. Czyczula¹⁷⁶, S. D'Auria⁵³,
 M. D'Onofrio⁷³, A. D'Orazio^{132a,132b}, M.J. Da Cunha Sargedas De Sousa^{124a}, C. Da Via⁸²,
 W. Dabrowski³⁷, A. Dafinca¹¹⁸, T. Dai⁸⁷, C. Dallapiccola⁸⁴, M. Dam³⁵, M. Dameri^{50a,50b},
 D.S. Damiani¹³⁷, H.O. Danielsson²⁹, V. Dao⁴⁹, G. Darbo^{50a}, G.L. Darlea^{25b}, W. Davey²⁰,
 T. Davidek¹²⁶, N. Davidson⁸⁶, R. Davidson⁷¹, E. Davies^{118,c}, M. Davies⁹³, A.R. Davison⁷⁷,
 Y. Davygora^{58a}, E. Dawe¹⁴², I. Dawson¹³⁹, R.K. Daya-Ishmukhametova²², K. De⁷,
 R. de Asmundis^{102a}, S. De Castro^{19a,19b}, S. De Cecco⁷⁸, J. de Graat⁹⁸, N. De Groot¹⁰⁴,
 P. de Jong¹⁰⁵, C. De La Taille¹¹⁵, H. De la Torre⁸⁰, F. De Lorenzi⁶³, L. de Mora⁷¹,
 L. De Nooij¹⁰⁵, D. De Pedis^{132a}, A. De Salvo^{132a}, U. De Sanctis^{164a,164c}, A. De Santo¹⁴⁹,
 J.B. De Vivie De Regie¹¹⁵, G. De Zorzi^{132a,132b}, W.J. Dearnaley⁷¹, R. Debbe²⁴,
 C. Debenedetti⁴⁵, B. Dechenaux⁵⁵, D.V. Dedovich⁶⁴, J. Degenhardt¹²⁰, C. Del Papa^{164a,164c},
 J. Del Peso⁸⁰, T. Del Prete^{122a,122b}, T. Delemontex⁵⁵, M. Deliyergiyev⁷⁴, A. Dell'Acqua²⁹,
 L. Dell'Asta²¹, M. Della Pietra^{102a,j}, D. della Volpe^{102a,102b}, M. Delmastro⁴, P.A. Delsart⁵⁵,
 C. Deluca¹⁰⁵, S. Demers¹⁷⁶, M. Demichev⁶⁴, B. Demirköz^{11,l}, J. Deng¹⁶³, S.P. Denisov¹²⁸,
 D. Derendarz³⁸, J.E. Derkaoui^{135d}, F. Derue⁷⁸, P. Dervan⁷³, K. Desch²⁰, E. Devetak¹⁴⁸,
 P.O. Deviveiros¹⁰⁵, A. Dewhurst¹²⁹, B. DeWilde¹⁴⁸, S. Dhaliwal¹⁵⁸, R. Dhullipudi^{24,m},
 A. Di Ciaccio^{133a,133b}, L. Di Ciaccio⁴, A. Di Girolamo²⁹, B. Di Girolamo²⁹,
 S. Di Luise^{134a,134b}, A. Di Mattia¹⁷³, B. Di Micco²⁹, R. Di Nardo⁴⁷, A. Di Simone^{133a,133b},
 R. Di Sipio^{19a,19b}, M.A. Diaz^{31a}, E.B. Diehl⁸⁷, J. Dietrich⁴¹, T.A. Dietzsch^{58a}, S. Diglio⁸⁶,
 K. Dindar Yagci³⁹, J. Dingfelder²⁰, F. Dinut^{25a}, C. Dionisi^{132a,132b}, P. Dita^{25a}, S. Dita^{25a},
 F. Dittus²⁹, F. Djama⁸³, T. Djobava^{51b}, M.A.B. do Vale^{23c}, A. Do Valle Wemans^{124a,n},
 T.K.O. Doan⁴, M. Dobbs⁸⁵, R. Dobinson^{29,*}, D. Dobos²⁹, E. Dobson^{29,o}, J. Dodd³⁴,
 C. Doglioni⁴⁹, T. Doherty⁵³, Y. Doi^{65,*}, J. Dolejsi¹²⁶, I. Dolenc⁷⁴, Z. Dolezal¹²⁶,
 B.A. Dolgoshein^{96,*}, T. Dohmae¹⁵⁵, M. Donadelli^{23d}, J. Donini³³, J. Dopke²⁹, A. Doria^{102a},
 A. Dos Anjos¹⁷³, A. Dotti^{122a,122b}, M.T. Dova⁷⁰, A.D. Doxiadis¹⁰⁵, A.T. Doyle⁵³, M. Dris⁹,
 J. Dubbert⁹⁹, S. Dube¹⁴, E. Duchovni¹⁷², G. Duckeck⁹⁸, A. Dudarev²⁹, F. Dudziak⁶³,

M. Dührssen²⁹, I.P. Duerdoth⁸², L. Duflot¹¹⁵, M-A. Dufour⁸⁵, M. Dunford²⁹,
H. Duran Yildiz^{3a}, R. Duxfield¹³⁹, M. Dwuznik³⁷, F. Dydak²⁹, M. Düren⁵², J. Ebke⁹⁸,
S. Eckweiler⁸¹, K. Edmonds⁸¹, C.A. Edwards⁷⁶, N.C. Edwards⁵³, W. Ehrenfeld⁴¹,
T. Eifert¹⁴³, G. Eigen¹³, K. Einsweiler¹⁴, E. Eisenhandler⁷⁵, T. Ekelof¹⁶⁶, M. El Kacimi^{135c},
M. Ellert¹⁶⁶, S. Elles⁴, F. Ellinghaus⁸¹, K. Ellis⁷⁵, N. Ellis²⁹, J. Elmsheuser⁹⁸, M. Elsing²⁹,
D. Emeliyanov¹²⁹, R. Engelmann¹⁴⁸, A. Engl⁹⁸, B. Epp⁶¹, A. Eppig⁸⁷, J. Erdmann⁵⁴,
A. Ereditato¹⁶, D. Eriksson^{146a}, J. Ernst¹, M. Ernst²⁴, J. Ernwein¹³⁶, D. Errede¹⁶⁵,
S. Errede¹⁶⁵, E. Ertel⁸¹, M. Escalier¹¹⁵, H. Esch⁴², C. Escobar¹²³, X. Espinal Curull¹¹,
B. Esposito⁴⁷, F. Etienne⁸³, A.I. Etievre¹³⁶, E. Etzion¹⁵³, D. Evangelakou⁵⁴, H. Evans⁶⁰,
L. Fabbri^{19a,19b}, C. Fabre²⁹, R.M. Fakhruddinov¹²⁸, S. Falciano^{132a}, Y. Fang¹⁷³,
M. Fantì^{89a,89b}, A. Farbin⁷, A. Farilla^{134a}, J. Farley¹⁴⁸, T. Farooque¹⁵⁸, S. Farrell¹⁶³,
S.M. Farrington¹¹⁸, P. Farthouat²⁹, P. Fassnacht²⁹, D. Fassouliotis⁸, B. Fatholahzadeh¹⁵⁸,
A. Favareto^{89a,89b}, L. Fayard¹¹⁵, S. Fazio^{36a,36b}, R. Febbraro³³, P. Federic^{144a}, O.L. Fedin¹²¹,
W. Fedorko⁸⁸, M. Fehling-Kaschek⁴⁸, L. Feligioni⁸³, D. Fellmann⁵, C. Feng^{32d}, E.J. Feng⁵,
A.B. Fenyuk¹²⁸, J. Ferencei^{144b}, W. Fernando⁵, S. Ferrag⁵³, J. Ferrando⁵³, V. Ferrara⁴¹,
A. Ferrari¹⁶⁶, P. Ferrari¹⁰⁵, R. Ferrari^{119a}, D.E. Ferreira de Lima⁵³, A. Ferrer¹⁶⁷,
D. Ferrere⁴⁹, C. Ferretti⁸⁷, A. Ferretto Parodi^{50a,50b}, M. Fiascaris³⁰, F. Fiedler⁸¹,
A. Filipčič⁷⁴, F. Filthaut¹⁰⁴, M. Fincke-Keeler¹⁶⁹, M.C.N. Fiolhais^{124a,h}, L. Fiorini¹⁶⁷,
A. Firan³⁹, G. Fischer⁴¹, M.J. Fisher¹⁰⁹, M. Flechl⁴⁸, I. Fleck¹⁴¹, J. Fleckner⁸¹,
P. Fleischmann¹⁷⁴, S. Fleischmann¹⁷⁵, T. Flick¹⁷⁵, A. Floderus⁷⁹, L.R. Flores Castillo¹⁷³,
M.J. Flowerdew⁹⁹, T. Fonseca Martin¹⁶, A. Formica¹³⁶, A. Forti⁸², D. Fortin^{159a},
D. Fournier¹¹⁵, H. Fox⁷¹, P. Francavilla¹¹, S. Franchino^{119a,119b}, D. Francis²⁹, T. Frank¹⁷²,
S. Franz²⁹, M. Fraternali^{119a,119b}, S. Fratina¹²⁰, S.T. French²⁷, C. Friedrich⁴¹,
F. Friedrich⁴³, R. Froeschl²⁹, D. Froidevaux²⁹, J.A. Frost²⁷, C. Fukunaga¹⁵⁶,
E. Fullana Torregrosa²⁹, B.G. Fulson¹⁴³, J. Fuster¹⁶⁷, C. Gabaldon²⁹, O. Gabizon¹⁷²,
T. Gadfort²⁴, S. Gadomski⁴⁹, G. Gagliardi^{50a,50b}, P. Gagnon⁶⁰, C. Galea⁹⁸, E.J. Gallas¹¹⁸,
V. Gallo¹⁶, B.J. Gallop¹²⁹, P. Gallus¹²⁵, K.K. Gan¹⁰⁹, Y.S. Gao^{143,e}, A. Gaponenko¹⁴,
F. Garberon¹⁷⁶, M. Garcia-Sciveres¹⁴, C. García¹⁶⁷, J.E. García Navarro¹⁶⁷,
R.W. Gardner³⁰, N. Garelli²⁹, H. Garitaonandia¹⁰⁵, V. Garonne²⁹, J. Garvey¹⁷, C. Gatti⁴⁷,
G. Gaudio^{119a}, B. Gaur¹⁴¹, L. Gauthier¹³⁶, P. Gauzzi^{132a,132b}, I.L. Gavrilenko⁹⁴, C. Gay¹⁶⁸,
G. Gaycken²⁰, E.N. Gazis⁹, P. Ge^{32d}, Z. Gecse¹⁶⁸, C.N.P. Gee¹²⁹, D.A.A. Geerts¹⁰⁵,
Ch. Geich-Gimbel²⁰, K. Gellerstedt^{146a,146b}, C. Gemme^{50a}, A. Gemmell⁵³, M.H. Genest⁵⁵,
S. Gentile^{132a,132b}, M. George⁵⁴, S. George⁷⁶, P. Gerlach¹⁷⁵, A. Gershon¹⁵³, C. Geweniger^{58a},
H. Ghazlane^{135b}, N. Ghodbane³³, B. Giacobbe^{19a}, S. Giagu^{132a,132b}, V. Giakoumopoulou⁸,
V. Giangiobbe¹¹, F. Gianotti²⁹, B. Gibbard²⁴, A. Gibson¹⁵⁸, S.M. Gibson²⁹, D. Gillberg²⁸,
A.R. Gillman¹²⁹, D.M. Gingrich^{2,d}, J. Ginzburg¹⁵³, N. Giokaris⁸, M.P. Giordani^{164c},
R. Giordano^{102a,102b}, F.M. Giorgi¹⁵, P. Giovannini⁹⁹, P.F. Giraud¹³⁶, D. Giugni^{89a},
M. Giunta⁹³, P. Giusti^{19a}, B.K. Gjelsten¹¹⁷, L.K. Gladilin⁹⁷, C. Glasman⁸⁰, J. Glatzer⁴⁸,
A. Glazov⁴¹, K.W. Glitza¹⁷⁵, G.L. Glonti⁶⁴, J.R. Goddard⁷⁵, J. Godfrey¹⁴², J. Godlewski²⁹,
M. Goebel⁴¹, T. Göpfert⁴³, C. Goeringer⁸¹, C. Gössling⁴², S. Goldfarb⁸⁷, T. Golling¹⁷⁶,
A. Gomes^{124a,b}, L.S. Gomez Fajardo⁴¹, R. Gonçalo⁷⁶,
J. Goncalves Pinto Firmino Da Costa⁴¹, L. Gonella²⁰, S. Gonzalez¹⁷³, S. González de la
Hoz¹⁶⁷, G. Gonzalez Parra¹¹, M.L. Gonzalez Silva²⁶, S. Gonzalez-Sevilla⁴⁹, J.J. Goodson¹⁴⁸,

L. Goossens²⁹, P.A. Gorbounov⁹⁵, H.A. Gordon²⁴, I. Gorelov¹⁰³, G. Gorfine¹⁷⁵, B. Gorini²⁹,
 E. Gorini^{72a,72b}, A. Gorišek⁷⁴, E. Gornicki³⁸, B. Gosdzik⁴¹, A.T. Goshaw⁵, M. Gosselink¹⁰⁵,
 M.I. Gostkin⁶⁴, I. Gough Eschrich¹⁶³, M. Gouighri^{135a}, D. Goujdami^{135c}, M.P. Goulette⁴⁹,
 A.G. Goussiou¹³⁸, C. Goy⁴, S. Gozpinar²², I. Grabowska-Bold³⁷, P. Grafström^{19a,19b},
 K.-J. Grahn⁴¹, F. Grancagnolo^{72a}, S. Grancagnolo¹⁵, V. Grassi¹⁴⁸, V. Gratchev¹²¹,
 N. Grau³⁴, H.M. Gray²⁹, J.A. Gray¹⁴⁸, E. Graziani^{134a}, O.G. Grebenyuk¹²¹,
 T. Greenshaw⁷³, Z.D. Greenwood^{24,m}, K. Gregersen³⁵, I.M. Gregor⁴¹, P. Grenier¹⁴³,
 J. Griffiths¹³⁸, N. Grigalashvili⁶⁴, A.A. Grillo¹³⁷, S. Grinstein¹¹, Y.V. Grishkevich⁹⁷,
 J.-F. Grivaz¹¹⁵, E. Gross¹⁷², J. Grosse-Knetter⁵⁴, J. Groth-Jensen¹⁷², K. Grybel¹⁴¹,
 D. Guest¹⁷⁶, C. Guicheney³³, A. Guida^{72a,72b}, S. Guindon⁵⁴, U. Gul⁵³, H. Guler^{85,p},
 J. Gunther¹²⁵, B. Guo¹⁵⁸, J. Guo³⁴, P. Gutierrez¹¹¹, N. Guttman¹⁵³, O. Gutzwiller¹⁷³,
 C. Guyot¹³⁶, C. Gwenlan¹¹⁸, C.B. Gwilliam⁷³, A. Haas¹⁴³, S. Haas²⁹, C. Haber¹⁴,
 H.K. Hadavand³⁹, D.R. Hadley¹⁷, P. Haefner²⁰, F. Hahn²⁹, S. Haider²⁹, Z. Hajduk³⁸,
 H. Hakobyan¹⁷⁷, D. Hall¹¹⁸, J. Haller⁵⁴, K. Hamacher¹⁷⁵, P. Hamal¹¹³, M. Hamer⁵⁴,
 A. Hamilton^{145b,q}, S. Hamilton¹⁶¹, L. Han^{32b}, K. Hanagaki¹¹⁶, K. Hanawa¹⁶⁰, M. Hance¹⁴,
 C. Handel⁸¹, P. Hanke^{58a}, J.R. Hansen³⁵, J.B. Hansen³⁵, J.D. Hansen³⁵, P.H. Hansen³⁵,
 P. Hansson¹⁴³, K. Hara¹⁶⁰, G.A. Hare¹³⁷, T. Harenberg¹⁷⁵, S. Harkusha⁹⁰, D. Harper⁸⁷,
 R.D. Harrington⁴⁵, O.M. Harris¹³⁸, J. Hartert⁴⁸, F. Hartjes¹⁰⁵, T. Haruyama⁶⁵,
 A. Harvey⁵⁶, S. Hasegawa¹⁰¹, Y. Hasegawa¹⁴⁰, S. Hassani¹³⁶, S. Haug¹⁶, M. Hauschild²⁹,
 R. Hauser⁸⁸, M. Havranek²⁰, C.M. Hawkes¹⁷, R.J. Hawkins²⁹, A.D. Hawkins⁷⁹,
 D. Hawkins¹⁶³, T. Hayakawa⁶⁶, T. Hayashi¹⁶⁰, D. Hayden⁷⁶, C.P. Hays¹¹⁸, H.S. Hayward⁷³,
 S.J. Haywood¹²⁹, M. He^{32d}, S.J. Head¹⁷, V. Hedberg⁷⁹, L. Heelan⁷, S. Heim⁸⁸,
 B. Heinemann¹⁴, S. Heisterkamp³⁵, L. Helary²¹, C. Heller⁹⁸, M. Heller²⁹,
 S. Hellman^{146a,146b}, D. Hellmich²⁰, C. Hensens¹¹, R.C.W. Henderson⁷¹, M. Henke^{58a},
 A. Henrichs⁵⁴, A.M. Henriques Correia²⁹, S. Henrot-Versille¹¹⁵, C. Hensel⁵⁴, T. Henß¹⁷⁵,
 C.M. Hernandez⁷, Y. Hernández Jiménez¹⁶⁷, R. Herrberg¹⁵, G. Herten⁴⁸,
 R. Hertenberger⁹⁸, L. Hervas²⁹, G.G. Hesketh⁷⁷, N.P. Hessey¹⁰⁵, E. Higón-Rodríguez¹⁶⁷,
 J.C. Hill²⁷, K.H. Hiller⁴¹, S. Hillert²⁰, S.J. Hillier¹⁷, I. Hinchliffe¹⁴, E. Hines¹²⁰,
 M. Hirose¹¹⁶, F. Hirsch⁴², D. Hirschbuehl¹⁷⁵, J. Hobbs¹⁴⁸, N. Hod¹⁵³, M.C. Hodgkinson¹³⁹,
 P. Hodgson¹³⁹, A. Hoecker²⁹, M.R. Hoferkamp¹⁰³, J. Hoffman³⁹, D. Hoffmann⁸³,
 M. Hohlfeld⁸¹, M. Holder¹⁴¹, S.O. Holmgren^{146a}, T. Holy¹²⁷, J.L. Holzbauer⁸⁸,
 T.M. Hong¹²⁰, L. Hooft van Huysduynen¹⁰⁸, C. Horn¹⁴³, S. Horner⁴⁸, J.-Y. Hostachy⁵⁵,
 S. Hou¹⁵¹, A. Hoummada^{135a}, J. Howard¹¹⁸, J. Howarth⁸², I. Hristova¹⁵, J. Hrivnac¹¹⁵,
 T. Hryn'ova⁴, P.J. Hsu⁸¹, S.-C. Hsu¹⁴, Z. Hubacek¹²⁷, F. Hubaut⁸³, F. Huegging²⁰,
 A. Huettmann⁴¹, T.B. Huffman¹¹⁸, E.W. Hughes³⁴, G. Hughes⁷¹, M. Huhtinen²⁹,
 M. Hurwitz¹⁴, U. Husemann⁴¹, N. Huseynov^{64,r}, J. Huston⁸⁸, J. Huth⁵⁷, G. Iacobucci⁴⁹,
 G. Iakovidis⁹, M. Ibbotson⁸², I. Ibragimov¹⁴¹, L. Iconomidou-Fayard¹¹⁵, J. Idarraga¹¹⁵,
 P. Iengo^{102a}, O. Igonkina¹⁰⁵, Y. Ikegami⁶⁵, M. Ikeno⁶⁵, D. Iliadis¹⁵⁴, N. Ilic¹⁵⁸, T. Ince²⁰,
 J. Inigo-Golfín²⁹, P. Ioannou⁸, M. Iodice^{134a}, K. Iordanidou⁸, V. Ippolito^{132a,132b},
 A. Irlés Quiles¹⁶⁷, C. Isaksson¹⁶⁶, M. Ishino⁶⁷, M. Ishitsuka¹⁵⁷, R. Ishmukhametov³⁹,
 C. Issever¹¹⁸, S. Istin^{18a}, A.V. Ivashin¹²⁸, W. Iwanski³⁸, H. Iwasaki⁶⁵, J.M. Izen⁴⁰,
 V. Izzo^{102a}, B. Jackson¹²⁰, J.N. Jackson⁷³, P. Jackson¹⁴³, M.R. Jaekel²⁹, V. Jain⁶⁰,
 K. Jakobs⁴⁸, S. Jakobsen³⁵, T. Jakoubek¹²⁵, J. Jakubek¹²⁷, D.K. Jana¹¹¹, E. Jansen⁷⁷,

H. Jansen²⁹, A. Jantsch⁹⁹, M. Janus⁴⁸, G. Jarlskog⁷⁹, L. Jeanty⁵⁷, I. Jen-La Plante³⁰,
 P. Jenni²⁹, A. Jeremie⁴, P. Jež³⁵, S. Jézéquel⁴, M.K. Jha^{19a}, H. Ji¹⁷³, W. Ji⁸¹, J. Jia¹⁴⁸,
 Y. Jiang^{32b}, M. Jimenez Belenguer⁴¹, S. Jin^{32a}, O. Jinnouchi¹⁵⁷, M.D. Joergensen³⁵,
 D. Joffe³⁹, M. Johansen^{146a,146b}, K.E. Johansson^{146a}, P. Johansson¹³⁹, S. Johnert⁴¹,
 K.A. Johns⁶, K. Jon-And^{146a,146b}, G. Jones¹⁷⁰, R.W.L. Jones⁷¹, T.J. Jones⁷³, C. Joram²⁹,
 P.M. Jorge^{124a}, K.D. Joshi⁸², J. Jovicevic¹⁴⁷, T. Jovin^{12b}, X. Ju¹⁷³, C.A. Jung⁴²,
 R.M. Jungst²⁹, V. Juranek¹²⁵, P. Jussel⁶¹, A. Juste Rozas¹¹, S. Kabana¹⁶, M. Kaci¹⁶⁷,
 A. Kaczmarska³⁸, P. Kadlecik³⁵, M. Kado¹¹⁵, H. Kagan¹⁰⁹, M. Kagan⁵⁷, E. Kajomovitz¹⁵²,
 S. Kalinin¹⁷⁵, L.V. Kalinovskaya⁶⁴, S. Kama³⁹, N. Kanaya¹⁵⁵, M. Kaneda²⁹, S. Kaneti²⁷,
 T. Kanno¹⁵⁷, V.A. Kantserov⁹⁶, J. Kanzaki⁶⁵, B. Kaplan¹⁷⁶, A. Kapliy³⁰, J. Kaplon²⁹,
 D. Kar⁵³, M. Karagounis²⁰, K. Karakostas⁹, M. Karnevskiy⁴¹, V. Kartvelishvili⁷¹,
 A.N. Karyukhin¹²⁸, L. Kashif¹⁷³, G. Kasieczka^{58b}, R.D. Kass¹⁰⁹, A. Kastanas¹³,
 M. Kataoka⁴, Y. Kataoka¹⁵⁵, E. Katsoufis⁹, J. Katzy⁴¹, V. Kaushik⁶, K. Kawagoe⁶⁹,
 T. Kawamoto¹⁵⁵, G. Kawamura⁸¹, M.S. Kayl¹⁰⁵, V.A. Kazanin¹⁰⁷, M.Y. Kazarinov⁶⁴,
 R. Keeler¹⁶⁹, R. Kehoe³⁹, M. Keil⁵⁴, G.D. Kekelidze⁶⁴, J.S. Keller¹³⁸, M. Kenyon⁵³,
 O. Kepka¹²⁵, N. Kerschen²⁹, B.P. Kerševan⁷⁴, S. Kersten¹⁷⁵, K. Kessoku¹⁵⁵, J. Keung¹⁵⁸,
 F. Khalil-zada¹⁰, H. Khandanyan¹⁶⁵, A. Khanov¹¹², D. Kharchenko⁶⁴, A. Khodinov⁹⁶,
 A. Khomich^{58a}, T.J. Khoo²⁷, G. Khoriauli²⁰, A. Khoroshilov¹⁷⁵, V. Khovanskiy⁹⁵,
 E. Khramov⁶⁴, J. Khubua^{51b}, H. Kim^{146a,146b}, S.H. Kim¹⁶⁰, N. Kimura¹⁷¹, O. Kind¹⁵,
 B.T. King⁷³, M. King⁶⁶, R.S.B. King¹¹⁸, J. Kirk¹²⁹, A.E. Kiryunin⁹⁹, T. Kishimoto⁶⁶,
 D. Kisielewska³⁷, T. Kittelmann¹²³, E. Kladiva^{144b}, M. Klein⁷³, U. Klein⁷³,
 K. Kleinknecht⁸¹, M. Klemetti⁸⁵, A. Klier¹⁷², P. Klimek^{146a,146b}, A. Klimentov²⁴,
 R. Klingenberg⁴², J.A. Klinger⁸², E.B. Klinkby³⁵, T. Klioutchnikova²⁹, P.F. Klok¹⁰⁴,
 S. Klous¹⁰⁵, E.-E. Kluge^{58a}, T. Kluge⁷³, P. Kluit¹⁰⁵, S. Kluth⁹⁹, N.S. Knecht¹⁵⁸,
 E. Kneringer⁶¹, E.B.F.G. Knoops⁸³, A. Knue⁵⁴, B.R. Ko⁴⁴, T. Kobayashi¹⁵⁵, M. Kobel⁴³,
 M. Kocian¹⁴³, P. Kodyš¹²⁶, K. Köneke²⁹, A.C. König¹⁰⁴, S. Koenig⁸¹, L. Köpke⁸¹,
 F. Koetsveld¹⁰⁴, P. Koevesarki²⁰, T. Koffas²⁸, E. Koffeman¹⁰⁵, L.A. Kogan¹¹⁸,
 S. Kohlmann¹⁷⁵, F. Kohn⁵⁴, Z. Kohout¹²⁷, T. Kohriki⁶⁵, T. Koi¹⁴³, G.M. Kolachev¹⁰⁷,
 H. Kolanoski¹⁵, V. Kolesnikov⁶⁴, I. Koletsou^{89a}, J. Koll⁸⁸, M. Kollefrath⁴⁸, A.A. Komar⁹⁴,
 Y. Komori¹⁵⁵, T. Kondo⁶⁵, T. Kono^{41,s}, A.I. Kononov⁴⁸, R. Konoplich^{108,t},
 N. Konstantinidis⁷⁷, S. Koperny³⁷, K. Korcyl³⁸, K. Kordas¹⁵⁴, A. Korn¹¹⁸, A. Korol¹⁰⁷,
 I. Korolkov¹¹, E.V. Korolkova¹³⁹, V.A. Korotkov¹²⁸, O. Kortner⁹⁹, S. Kortner⁹⁹,
 V.V. Kostyukhin²⁰, S. Kotov⁹⁹, V.M. Kotov⁶⁴, A. Kotwal⁴⁴, C. Kourkoumelis⁸,
 V. Kouskoura¹⁵⁴, A. Koutsman^{159a}, R. Kowalewski¹⁶⁹, T.Z. Kowalski³⁷, W. Kozanecki¹³⁶,
 A.S. Kozhin¹²⁸, V. Kral¹²⁷, V.A. Kramarenko⁹⁷, G. Kramberger⁷⁴, M.W. Krasny⁷⁸,
 A. Krasznahorkay¹⁰⁸, J. Kraus⁸⁸, J.K. Kraus²⁰, S. Kreiss¹⁰⁸, F. Krejci¹²⁷, J. Kretzschmar⁷³,
 N. Krieger⁵⁴, P. Krieger¹⁵⁸, K. Kroeninger⁵⁴, H. Kroha⁹⁹, J. Kroll¹²⁰, J. Kroseberg²⁰,
 J. Krstic^{12a}, U. Kruchonak⁶⁴, H. Krüger²⁰, T. Kruker¹⁶, N. Krumnack⁶³,
 Z.V. KrumshTEYN⁶⁴, A. Kruth²⁰, T. Kubota⁸⁶, S. Kудay^{3a}, S. Kuehn⁴⁸, A. Kugel^{58c},
 T. Kuhl⁴¹, D. Kuhn⁶¹, V. Kukhtin⁶⁴, Y. Kulchitsky⁹⁰, S. Kuleshov^{31b}, C. Kummer⁹⁸,
 M. Kuna⁷⁸, J. Kunkle¹²⁰, A. Kupco¹²⁵, H. Kurashige⁶⁶, M. Kurata¹⁶⁰, Y.A. Kurochkin⁹⁰,
 V. Kus¹²⁵, E.S. Kuwertz¹⁴⁷, M. Kuze¹⁵⁷, J. Kvita¹⁴², R. Kwee¹⁵, A. La Rosa⁴⁹,
 L. La Rotonda^{36a,36b}, L. Labarga⁸⁰, J. Labbe⁴, S. Lablak^{135a}, C. Lacasta¹⁶⁷,

F. Lacava^{132a,132b}, H. Lacker¹⁵, D. Lacour⁷⁸, V.R. Lacuesta¹⁶⁷, E. Ladygin⁶⁴, R. Lafaye⁴,
 B. Laforge⁷⁸, T. Lagouri⁸⁰, S. Lai⁴⁸, E. Laisne⁵⁵, M. Lamanna²⁹, L. Lambourne⁷⁷,
 C.L. Lampen⁶, W. Lampl⁶, E. Lancon¹³⁶, U. Landgraf⁴⁸, M.P.J. Landon⁷⁵, J.L. Lane⁸²,
 V.S. Lang^{58a}, C. Lange⁴¹, A.J. Lankford¹⁶³, F. Lanni²⁴, K. Lantzsche¹⁷⁵, S. Laplace⁷⁸,
 C. Lapoire²⁰, J.F. Laporte¹³⁶, T. Lari^{89a}, A. Larner¹¹⁸, M. Lassnig²⁹, P. Laurelli⁴⁷,
 V. Lavorini^{36a,36b}, W. Lavrijsen¹⁴, P. Laycock⁷³, O. Le Dortz⁷⁸, E. Le Guirriec⁸³,
 C. Le Maner¹⁵⁸, E. Le Menedeu¹¹, T. LeCompte⁵, F. Ledroit-Guillon⁵⁵, H. Lee¹⁰⁵,
 J.S.H. Lee¹¹⁶, S.C. Lee¹⁵¹, L. Lee¹⁷⁶, M. Lefebvre¹⁶⁹, M. Legendre¹³⁶, F. Legger⁹⁸,
 C. Leggett¹⁴, M. Lehmacher²⁰, G. Lehmann Miotto²⁹, X. Lei⁶, M.A.L. Leite^{23d},
 R. Leitner¹²⁶, D. Lellouch¹⁷², B. Lemmer⁵⁴, V. Lendermann^{58a}, K.J.C. Leney^{145b},
 T. Lenz¹⁰⁵, G. Lenzen¹⁷⁵, B. Lenzi²⁹, K. Leonhardt⁴³, S. Leontsinis⁹, F. Lepold^{58a},
 C. Leroy⁹³, J-R. Lessard¹⁶⁹, C.G. Lester²⁷, C.M. Lester¹²⁰, J. Levêque⁴, D. Levin⁸⁷,
 L.J. Levinson¹⁷², A. Lewis¹¹⁸, G.H. Lewis¹⁰⁸, A.M. Leyko²⁰, M. Leyton¹⁵, B. Li⁸³,
 H. Li^{173,u}, S. Li^{32b,v}, X. Li⁸⁷, Z. Liang^{118,w}, H. Liao³³, B. Liberti^{133a}, P. Lichard²⁹,
 M. Lichtnecker⁹⁸, K. Lie¹⁶⁵, W. Liebig¹³, C. Limbach²⁰, A. Limosani⁸⁶, M. Limper⁶²,
 S.C. Lin^{151,x}, F. Linde¹⁰⁵, J.T. Linnemann⁸⁸, E. Lipeles¹²⁰, A. Lipniacka¹³, T.M. Liss¹⁶⁵,
 D. Lissauer²⁴, A. Lister⁴⁹, A.M. Litke¹³⁷, C. Liu²⁸, D. Liu¹⁵¹, H. Liu⁸⁷, J.B. Liu⁸⁷, L. Liu⁸⁷,
 M. Liu^{32b}, Y. Liu^{32b}, M. Livan^{119a,119b}, S.S.A. Livermore¹¹⁸, A. Lleres⁵⁵,
 J. Llorente Merino⁸⁰, S.L. Lloyd⁷⁵, E. Lobodzinska⁴¹, P. Loch⁶, W.S. Lockman¹³⁷,
 T. Loddenkoetter²⁰, F.K. Loebinger⁸², A. Loginov¹⁷⁶, C.W. Loh¹⁶⁸, T. Lohse¹⁵,
 K. Lohwasser⁴⁸, M. Lokajicek¹²⁵, V.P. Lombardo⁴, R.E. Long⁷¹, L. Lopes^{124a},
 D. Lopez Mateos⁵⁷, J. Lorenz⁹⁸, N. Lorenzo Martinez¹¹⁵, M. Losada¹⁶², P. Loscutoff¹⁴,
 F. Lo Sterzo^{132a,132b}, M.J. Losty^{159a}, X. Lou⁴⁰, A. Lounis¹¹⁵, K.F. Loureiro¹⁶², J. Love²¹,
 P.A. Love⁷¹, A.J. Lowe^{143,e}, F. Lu^{32a}, H.J. Lubatti¹³⁸, C. Luci^{132a,132b}, A. Lucotte⁵⁵,
 A. Ludwig⁴³, D. Ludwig⁴¹, I. Ludwig⁴⁸, J. Ludwig⁴⁸, F. Luehring⁶⁰, G. Luijckx¹⁰⁵,
 W. Lukas⁶¹, D. Lumb⁴⁸, L. Luminari^{132a}, E. Lund¹¹⁷, B. Lund-Jensen¹⁴⁷, B. Lundberg⁷⁹,
 J. Lundberg^{146a,146b}, O. Lundberg^{146a,146b}, J. Lundquist³⁵, M. Lungwitz⁸¹, D. Lynn²⁴,
 E. Lytken⁷⁹, H. Ma²⁴, L.L. Ma¹⁷³, G. Maccarrone⁴⁷, A. Macchiolo⁹⁹, B. Maček⁷⁴,
 J. Machado Miguens^{124a}, R. Mackeprang³⁵, R.J. Madaras¹⁴, W.F. Mader⁴³, R. Maenner^{58c},
 T. Maeno²⁴, P. Mättig¹⁷⁵, S. Mättig⁴¹, L. Magnoni²⁹, E. Magradze⁵⁴, K. Mahboubi⁴⁸,
 S. Mahmoud⁷³, G. Mahout¹⁷, C. Maiani¹³⁶, C. Maidantchik^{23a}, A. Maio^{124a,b},
 S. Majewski²⁴, Y. Makida⁶⁵, N. Makovec¹¹⁵, P. Mal¹³⁶, B. Malaescu²⁹, Pa. Malecki³⁸,
 P. Malecki³⁸, V.P. Maleev¹²¹, F. Malek⁵⁵, U. Mallik⁶², D. Malon⁵, C. Malone¹⁴³,
 S. Maltezos⁹, V. Malyshev¹⁰⁷, S. Malyukov²⁹, R. Mameghani⁹⁸, J. Mamuzic^{12b},
 A. Manabe⁶⁵, L. Mandelli^{89a}, I. Mandić⁷⁴, R. Mandrysch¹⁵, J. Maneira^{124a},
 P.S. Manguard⁸⁸, L. Manhaes de Andrade Filho^{23a}, A. Mann⁵⁴, P.M. Manning¹³⁷,
 A. Manousakis-Katsikakis⁸, B. Mansoulie¹³⁶, A. Mapelli²⁹, L. Mapelli²⁹, L. March⁸⁰,
 J.F. Marchand²⁸, F. Marchese^{133a,133b}, G. Marchiori⁷⁸, M. Marcisovsky¹²⁵, C.P. Marino¹⁶⁹,
 F. Marroquim^{23a}, Z. Marshall²⁹, F.K. Martens¹⁵⁸, L.F. Marti¹⁶, S. Marti-Garcia¹⁶⁷,
 B. Martin²⁹, B. Martin⁸⁸, J.P. Martin⁹³, T.A. Martin¹⁷, V.J. Martin⁴⁵,
 B. Martin dit Latour⁴⁹, S. Martin-Haugh¹⁴⁹, M. Martinez¹¹, V. Martinez Outschoorn⁵⁷,
 A.C. Martyniuk¹⁶⁹, M. Marx⁸², F. Marzano^{132a}, A. Marzin¹¹¹, L. Masetti⁸¹, T. Mashimo¹⁵⁵,
 R. Mashinistov⁹⁴, J. Masik⁸², A.L. Maslennikov¹⁰⁷, I. Massa^{19a,19b}, G. Massaro¹⁰⁵,

N. Massol⁴, A. Mastroberardino^{36a,36b}, T. Masubuchi¹⁵⁵, P. Matricon¹¹⁵, H. Matsunaga¹⁵⁵,
 T. Matsushita⁶⁶, C. Mattravers^{118,c}, J. Maurer⁸³, S.J. Maxfield⁷³, A. Mayne¹³⁹,
 R. Mazini¹⁵¹, M. Mazur²⁰, L. Mazzaferro^{133a,133b}, M. Mazzanti^{89a}, S.P. Mc Kee⁸⁷,
 A. McCarn¹⁶⁵, R.L. McCarthy¹⁴⁸, T.G. McCarthy²⁸, N.A. McCubbin¹²⁹,
 K.W. McFarlane⁵⁶, J.A. Mcfayden¹³⁹, H. McGlone⁵³, G. Mchedlidze^{51b}, T. Mclaughlan¹⁷,
 S.J. McMahon¹²⁹, R.A. McPherson^{169,k}, A. Meade⁸⁴, J. Mechnich¹⁰⁵, M. Mechtel¹⁷⁵,
 M. Medinnis⁴¹, R. Meera-Lebbai¹¹¹, T. Meguro¹¹⁶, R. Mehdiyev⁹³, S. Mehlhase³⁵,
 A. Mehta⁷³, K. Meier^{58a}, B. Meirose⁷⁹, C. Melachrinou³⁰, B.R. Mellado Garcia¹⁷³,
 F. Meloni^{89a,89b}, L. Mendoza Navas¹⁶², Z. Meng^{151,u}, A. Mengarelli^{19a,19b}, S. Menke⁹⁹,
 E. Meoni¹⁶¹, K.M. Mercurio⁵⁷, P. Mermod⁴⁹, L. Merola^{102a,102b}, C. Meroni^{89a},
 F.S. Merritt³⁰, H. Merritt¹⁰⁹, A. Messina^{29,y}, J. Metcalfe¹⁰³, A.S. Mete¹⁶³, C. Meyer⁸¹,
 C. Meyer³⁰, J-P. Meyer¹³⁶, J. Meyer¹⁷⁴, J. Meyer⁵⁴, T.C. Meyer²⁹, W.T. Meyer⁶³,
 J. Miao^{32d}, S. Michal²⁹, L. Micu^{25a}, R.P. Middleton¹²⁹, S. Migas⁷³, L. Mijović⁴¹,
 G. Mikenberg¹⁷², M. Mikestikova¹²⁵, M. Mikuž⁷⁴, D.W. Miller³⁰, R.J. Miller⁸⁸,
 W.J. Mills¹⁶⁸, C. Mills⁵⁷, A. Milov¹⁷², D.A. Milstead^{146a,146b}, D. Milstein¹⁷²,
 A.A. Minaenko¹²⁸, M. Miñano Moya¹⁶⁷, I.A. Minashvili⁶⁴, A.I. Mincer¹⁰⁸, B. Mindur³⁷,
 M. Mineev⁶⁴, Y. Ming¹⁷³, L.M. Mir¹¹, G. Mirabelli^{132a}, J. Mitrevski¹³⁷, V.A. Mitsou¹⁶⁷,
 S. Mitsui⁶⁵, P.S. Miyagawa¹³⁹, J.U. Mjörnmark⁷⁹, T. Moa^{146a,146b}, V. Moeller²⁷, K. Mönig⁴¹,
 N. Möser²⁰, S. Mohapatra¹⁴⁸, W. Mohr⁴⁸, R. Moles-Valls¹⁶⁷, J. Monk⁷⁷, E. Monnier⁸³,
 J. Montejo Berlingen¹¹, S. Montesano^{89a,89b}, F. Monticelli⁷⁰, S. Monzani^{19a,19b},
 R.W. Moore², G.F. Moorhead⁸⁶, C. Mora Herrera⁴⁹, A. Moraes⁵³, N. Morange¹³⁶,
 J. Morel⁵⁴, G. Morello^{36a,36b}, D. Moreno⁸¹, M. Moreno Llácer¹⁶⁷, P. Morettini^{50a},
 M. Morgenstern⁴³, M. Morii⁵⁷, A.K. Morley²⁹, G. Mornacchi²⁹, J.D. Morris⁷⁵, L. Morvaj¹⁰¹,
 H.G. Moser⁹⁹, M. Mosidze^{51b}, J. Moss¹⁰⁹, R. Mount¹⁴³, E. Mountricha^{9,z},
 S.V. Mouraviev⁹⁴, E.J.W. Moyse⁸⁴, F. Mueller^{58a}, J. Mueller¹²³, K. Mueller²⁰,
 T.A. Müller⁹⁸, T. Mueller⁸¹, D. Muenstermann²⁹, Y. Munwes¹⁵³, W.J. Murray¹²⁹,
 I. Mussche¹⁰⁵, E. Musto^{102a,102b}, A.G. Myagkov¹²⁸, M. Myska¹²⁵, J. Nadal¹¹, K. Nagai¹⁶⁰,
 K. Nagano⁶⁵, A. Nagarkar¹⁰⁹, Y. Nagasaka⁵⁹, M. Nagel⁹⁹, A.M. Nairz²⁹, Y. Nakahama²⁹,
 K. Nakamura¹⁵⁵, T. Nakamura¹⁵⁵, I. Nakano¹¹⁰, G. Nanava²⁰, A. Napier¹⁶¹, R. Narayan^{58b},
 M. Nash^{77,c}, T. Nattermann²⁰, T. Naumann⁴¹, G. Navarro¹⁶², H.A. Neal⁸⁷,
 P.Yu. Nechaeva⁹⁴, T.J. Neep⁸², A. Negri^{119a,119b}, G. Negri²⁹, S. Nektarijevic⁴⁹, A. Nelson¹⁶³,
 T.K. Nelson¹⁴³, S. Nemecek¹²⁵, P. Nemethy¹⁰⁸, A.A. Nepomuceno^{23a}, M. Nessi^{29,aa},
 M.S. Neubauer¹⁶⁵, A. Neusiedl⁸¹, R.M. Neves¹⁰⁸, P. Nevski²⁴, P.R. Newman¹⁷,
 V. Nguyen Thi Hong¹³⁶, R.B. Nickerson¹¹⁸, R. Nicolaidou¹³⁶, B. Nicquevert²⁹,
 F. Niedercorn¹¹⁵, J. Nielsen¹³⁷, N. Nikiforou³⁴, A. Nikiforov¹⁵, V. Nikolaenko¹²⁸,
 I. Nikolic-Audit⁷⁸, K. Nikolics⁴⁹, K. Nikolopoulos²⁴, H. Nilsen⁴⁸, P. Nilsson⁷,
 Y. Ninomiya¹⁵⁵, A. Nisati^{132a}, R. Nisius⁹⁹, T. Nobe¹⁵⁷, L. Nodulman⁵, M. Nomachi¹¹⁶,
 I. Nomidis¹⁵⁴, M. Nordberg²⁹, P.R. Norton¹²⁹, J. Novakova¹²⁶, M. Nozaki⁶⁵, L. Nozka¹¹³,
 I.M. Nugent^{159a}, A.-E. Nuncio-Quiroz²⁰, G. Nunes Hanninger⁸⁶, T. Nunnemann⁹⁸,
 E. Nurse⁷⁷, B.J. O'Brien⁴⁵, S.W. O'Neale^{17,*}, D.C. O'Neil¹⁴², V. O'Shea⁵³, L.B. Oakes⁹⁸,
 F.G. Oakham^{28,d}, H. Oberlack⁹⁹, J. Ocariz⁷⁸, A. Ochi⁶⁶, S. Oda⁶⁹, S. Odaka⁶⁵, J. Odier⁸³,
 H. Ogren⁶⁰, A. Oh⁸², S.H. Oh⁴⁴, C.C. Ohm^{146a,146b}, T. Ohshima¹⁰¹, H. Okawa¹⁶³,
 Y. Okumura³⁰, T. Okuyama¹⁵⁵, A. Olariu^{25a}, A.G. Olchevski⁶⁴, S.A. Olivares Pino^{31a},

M. Oliveira^{124a,h}, D. Oliveira Damazio²⁴, E. Oliver Garcia¹⁶⁷, D. Olivito¹²⁰, A. Olszewski³⁸,
J. Olszowska³⁸, A. Onofre^{124a,ab}, P.U.E. Onyisi³⁰, C.J. Oram^{159a}, M.J. Oreglia³⁰,
Y. Oren¹⁵³, D. Orestano^{134a,134b}, N. Orlando^{72a,72b}, I. Orlov¹⁰⁷, C. Oropeza Barrera⁵³,
R.S. Orr¹⁵⁸, B. Osculati^{50a,50b}, R. Ospanov¹²⁰, C. Osuna¹¹, G. Otero y Garzon²⁶,
J.P. Ottersbach¹⁰⁵, M. Ouchrif^{135d}, E.A. Ouellette¹⁶⁹, F. Ould-Saada¹¹⁷, A. Ouraou¹³⁶,
Q. Ouyang^{32a}, A. Ovcharova¹⁴, M. Owen⁸², S. Owen¹³⁹, V.E. Ozcan^{18a}, N. Ozturk⁷,
A. Pacheco Pages¹¹, C. Padilla Aranda¹¹, S. Pagan Griso¹⁴, E. Paganis¹³⁹, F. Paige²⁴,
P. Pais⁸⁴, K. Pajchel¹¹⁷, G. Palacino^{159b}, C.P. Paleari⁶, S. Palestini²⁹, D. Pallin³³,
A. Palma^{124a}, J.D. Palmer¹⁷, Y.B. Pan¹⁷³, E. Panagiotopoulou⁹, P. Pani¹⁰⁵,
N. Panikashvili⁸⁷, S. Panitkin²⁴, D. Pantea^{25a}, A. Papadelis^{146a}, Th.D. Papadopoulou⁹,
A. Paramonov⁵, D. Paredes Hernandez³³, W. Park^{24,ac}, M.A. Parker²⁷, F. Parodi^{50a,50b},
J.A. Parsons³⁴, U. Parzefall⁴⁸, S. Pashapour⁵⁴, E. Pasqualucci^{132a}, S. Passaggio^{50a},
A. Passeri^{134a}, F. Pastore^{134a,134b}, Fr. Pastore⁷⁶, G. Pásztor^{49,ad}, S. Pataraiia¹⁷⁵, N. Patel¹⁵⁰,
J.R. Pater⁸², S. Patricelli^{102a,102b}, T. Pauly²⁹, M. Pecsny^{144a}, M.I. Pedraza Morales¹⁷³,
S.V. Peleganchuk¹⁰⁷, D. Pelikan¹⁶⁶, H. Peng^{32b}, B. Penning³⁰, A. Penson³⁴, J. Penwell⁶⁰,
M. Perantoni^{23a}, K. Perez^{34,ae}, T. Perez Cavalcanti⁴¹, E. Perez Codina^{159a}, M.T. Pérez
García-Estañ¹⁶⁷, V. Perez Reale³⁴, L. Perini^{89a,89b}, H. Pernegger²⁹, R. Perrino^{72a},
P. Perrodo⁴, V.D. Peshekhonov⁶⁴, K. Peters²⁹, B.A. Petersen²⁹, J. Petersen²⁹,
T.C. Petersen³⁵, E. Petit⁴, A. Petridis¹⁵⁴, C. Petridou¹⁵⁴, E. Petrolo^{132a},
F. Petrucci^{134a,134b}, D. Petschull⁴¹, M. Petteni¹⁴², R. Pezoa^{31b}, A. Phan⁸⁶, P.W. Phillips¹²⁹,
G. Piacquadio²⁹, A. Picazio⁴⁹, E. Piccaro⁷⁵, M. Piccinini^{19a,19b}, S.M. Piec⁴¹, R. Piegaia²⁶,
D.T. Pignotti¹⁰⁹, J.E. Pilcher³⁰, A.D. Pilkington⁸², J. Pina^{124a,b}, M. Pinamonti^{164a,164c},
A. Pinder¹¹⁸, J.L. Pinfold², B. Pinto^{124a}, C. Pizio^{89a,89b}, M. Plamondon¹⁶⁹, M.-A. Pleier²⁴,
E. Plotnikova⁶⁴, A. Poblaguev²⁴, S. Poddar^{58a}, F. Podlyski³³, L. Poggioli¹¹⁵,
T. Poghosyan²⁰, M. Pohl⁴⁹, G. Polesello^{119a}, A. Policicchio^{36a,36b}, A. Polini^{19a}, J. Poll⁷⁵,
V. Polychronakos²⁴, D. Pomeroy²², K. Pommès²⁹, L. Pontecorvo^{132a}, B.G. Pope⁸⁸,
G.A. Popeneciu^{25a}, D.S. Popovic^{12a}, A. Poppleton²⁹, X. Portell Bueso²⁹, G.E. Pospelov⁹⁹,
S. Pospisil¹²⁷, I.N. Potrap⁹⁹, C.J. Potter¹⁴⁹, C.T. Potter¹¹⁴, G. Poulard²⁹, J. Poveda⁶⁰,
V. Pozdnyakov⁶⁴, R. Prabhu⁷⁷, P. Pralavorio⁸³, A. Pranko¹⁴, S. Prasad²⁹, R. Pravahan²⁴,
S. Prell⁶³, K. Pretzl¹⁶, D. Price⁶⁰, J. Price⁷³, L.E. Price⁵, D. Prieur¹²³, M. Primavera^{72a},
K. Prokofiev¹⁰⁸, F. Prokoshin^{31b}, S. Protopopescu²⁴, J. Proudfoot⁵, X. Prudent⁴³,
M. Przybycien³⁷, H. Przysiezniak⁴, S. Psoroulas²⁰, E. Ptacek¹¹⁴, E. Pueschel⁸⁴,
J. Purdham⁸⁷, M. Purohit^{24,ac}, P. Puzo¹¹⁵, Y. Pylypchenko⁶², J. Qian⁸⁷, A. Quadt⁵⁴,
D.R. Quarrie¹⁴, W.B. Quayle¹⁷³, F. Quinonez^{31a}, M. Raas¹⁰⁴, V. Radescu⁴¹, P. Radloff¹¹⁴,
T. Rador^{18a}, F. Ragusa^{89a,89b}, G. Rahal¹⁷⁸, A.M. Rahimi¹⁰⁹, D. Rahm²⁴, S. Rajagopalan²⁴,
M. Rammensee⁴⁸, M. Rammes¹⁴¹, A.S. Randle-Conde³⁹, K. Randrianarivony²⁸,
F. Rauscher⁹⁸, T.C. Rave⁴⁸, M. Raymond²⁹, A.L. Read¹¹⁷, D.M. Rebuzzi^{119a,119b},
A. Redelbach¹⁷⁴, G. Redlinger²⁴, R. Reece¹²⁰, K. Reeves⁴⁰, E. Reinherz-Aronis¹⁵³,
A. Reinsch¹¹⁴, I. Reisinger⁴², C. Rembser²⁹, Z.L. Ren¹⁵¹, A. Renaud¹¹⁵, M. Rescigno^{132a},
S. Resconi^{89a}, B. Resende¹³⁶, P. Reznicek⁹⁸, R. Rezvani¹⁵⁸, R. Richter⁹⁹,
E. Richter-Was^{4,af}, M. Ridel⁷⁸, M. Rijpstra¹⁰⁵, M. Rijssenbeek¹⁴⁸, A. Rimoldi^{119a,119b},
L. Rinaldi^{19a}, R.R. Rios³⁹, I. Riu¹¹, G. Rivoltella^{89a,89b}, F. Rizatdinova¹¹², E. Rizvi⁷⁵,
S.H. Robertson^{85,k}, A. Robichaud-Veronneau¹¹⁸, D. Robinson²⁷, J.E.M. Robinson⁷⁷,

A. Robson⁵³, J.G. Rocha de Lima¹⁰⁶, C. Roda^{122a,122b}, D. Roda Dos Santos²⁹, A. Roe⁵⁴,
 S. Roe²⁹, O. Røhne¹¹⁷, S. Rolli¹⁶¹, A. Romaniouk⁹⁶, M. Romano^{19a,19b}, G. Romeo²⁶,
 E. Romero Adam¹⁶⁷, L. Roos⁷⁸, E. Ros¹⁶⁷, S. Rosati^{132a}, K. Rosbach⁴⁹, A. Rose¹⁴⁹,
 M. Rose⁷⁶, G.A. Rosenbaum¹⁵⁸, E.I. Rosenberg⁶³, P.L. Rosendahl¹³, O. Rosenthal¹⁴¹,
 L. Rosselet⁴⁹, V. Rossetti¹¹, E. Rossi^{132a,132b}, L.P. Rossi^{50a}, M. Rotaru^{25a}, I. Roth¹⁷²,
 J. Rothberg¹³⁸, D. Rousseau¹¹⁵, C.R. Royon¹³⁶, A. Rozanov⁸³, Y. Rozen¹⁵², X. Ruan^{32a,ag},
 F. Rubbo¹¹, I. Rubinskiy⁴¹, B. Ruckert⁹⁸, N. Ruckstuhl¹⁰⁵, V.I. Rud⁹⁷, C. Rudolph⁴³,
 G. Rudolph⁶¹, F. Rühr⁶, A. Ruiz-Martinez⁶³, L. Rumyantsev⁶⁴, Z. Rurikova⁴⁸,
 N.A. Rusakovich⁶⁴, J.P. Rutherford⁶, C. Ruwiedel¹⁴, P. Ruzicka¹²⁵, Y.F. Ryabov¹²¹,
 P. Ryan⁸⁸, M. Rybar¹²⁶, G. Rybkin¹¹⁵, N.C. Ryder¹¹⁸, A.F. Saavedra¹⁵⁰, I. Sadeh¹⁵³,
 H.F-W. Sadrozinski¹³⁷, R. Sadykov⁶⁴, F. Safai Tehrani^{132a}, H. Sakamoto¹⁵⁵,
 G. Salamanna⁷⁵, A. Salamon^{133a}, M. Saleem¹¹¹, D. Salek²⁹, D. Salihagic⁹⁹, A. Salnikov¹⁴³,
 J. Salt¹⁶⁷, B.M. Salvachua Ferrando⁵, D. Salvatore^{36a,36b}, F. Salvatore¹⁴⁹, A. Salvucci¹⁰⁴,
 A. Salzburger²⁹, D. Sampsonidis¹⁵⁴, B.H. Samset¹¹⁷, A. Sanchez^{102a,102b},
 V. Sanchez Martinez¹⁶⁷, H. Sandaker¹³, H.G. Sander⁸¹, M.P. Sanders⁹⁸, M. Sandhoff¹⁷⁵,
 T. Sandoval²⁷, C. Sandoval¹⁶², R. Sandstroem⁹⁹, D.P.C. Sankey¹²⁹, A. Sansoni⁴⁷,
 C. Santamarina Rios⁸⁵, C. Santoni³³, R. Santonico^{133a,133b}, H. Santos^{124a}, J.G. Saraiva^{124a},
 T. Sarangi¹⁷³, E. Sarkisyan-Grinbaum⁷, F. Sarri^{122a,122b}, G. Sartisohn¹⁷⁵, O. Sasaki⁶⁵,
 N. Sasao⁶⁷, I. Satsounkevitch⁹⁰, G. Sauvage⁴, E. Sauvan⁴, J.B. Sauvan¹¹⁵, P. Savard^{158,d},
 V. Savinov¹²³, D.O. Savu²⁹, L. Sawyer^{24,m}, D.H. Saxon⁵³, J. Saxon¹²⁰, C. Sbarra^{19a},
 A. Sbrizzi^{19a,19b}, O. Scallon⁹³, D.A. Scannicchio¹⁶³, M. Scarcella¹⁵⁰, J. Schaarschmidt¹¹⁵,
 P. Schacht⁹⁹, D. Schaefer¹²⁰, U. Schäfer⁸¹, S. Schaepe²⁰, S. Schaetzel^{158b}, A.C. Schaffer¹¹⁵,
 D. Schaile⁹⁸, R.D. Schamberger¹⁴⁸, A.G. Schamov¹⁰⁷, V. Scharf^{58a}, V.A. Schegelsky¹²¹,
 D. Scheirich⁸⁷, M. Schernau¹⁶³, M.I. Scherzer³⁴, C. Schiavi^{50a,50b}, J. Schieck⁹⁸,
 M. Schioppa^{36a,36b}, S. Schlenker²⁹, E. Schmidt⁴⁸, K. Schmieden²⁰, C. Schmitt⁸¹,
 S. Schmitt^{58b}, M. Schmitz²⁰, B. Schneider¹⁶, U. Schnoor⁴³, A. Schöning^{58b},
 A.L.S. Schorlemmer⁵⁴, M. Schott²⁹, D. Schouten^{159a}, J. Schovancova¹²⁵, M. Schram⁸⁵,
 C. Schroeder⁸¹, N. Schroer^{58c}, M.J. Schultens²⁰, J. Schultes¹⁷⁵, H.-C. Schultz-Coulon^{58a},
 H. Schulz¹⁵, M. Schumacher⁴⁸, B.A. Schumm¹³⁷, Ph. Schune¹³⁶, C. Schwanenberger⁸²,
 A. Schwartzman¹⁴³, Ph. Schwemling⁷⁸, R. Schwienhorst⁸⁸, R. Schwierz⁴³, J. Schwindling¹³⁶,
 T. Schwindt²⁰, M. Schwoerer⁴, G. Sciolla²², W.G. Scott¹²⁹, J. Searcy¹¹⁴, G. Sedov⁴¹,
 E. Sedykh¹²¹, S.C. Seidel¹⁰³, A. Seiden¹³⁷, F. Seifert⁴³, J.M. Seixas^{23a}, G. Sekhniaidze^{102a},
 S.J. Sekula³⁹, K.E. Selbach⁴⁵, D.M. Seliverstov¹²¹, B. Sellden^{146a}, G. Sellers⁷³,
 M. Seman^{144b}, N. Semprini-Cesari^{19a,19b}, C. Serfon⁹⁸, L. Serin¹¹⁵, L. Serkin⁵⁴, R. Seuster⁹⁹,
 H. Severini¹¹¹, A. Sfyrla²⁹, E. Shabalina⁵⁴, M. Shamim¹¹⁴, L.Y. Shan^{32a}, J.T. Shank²¹,
 Q.T. Shao⁸⁶, M. Shapiro¹⁴, P.B. Shatalov⁹⁵, K. Shaw^{164a,164c}, D. Sherman¹⁷⁶,
 P. Sherwood⁷⁷, A. Shibata¹⁰⁸, S. Shimizu²⁹, M. Shimojima¹⁰⁰, T. Shin⁵⁶, M. Shiyakova⁶⁴,
 A. Shmeleva⁹⁴, M.J. Shochet³⁰, D. Short¹¹⁸, S. Shrestha⁶³, E. Shulga⁹⁶, M.A. Shupe⁶,
 P. Sicho¹²⁵, A. Sidoti^{132a}, F. Siegert⁴⁸, Dj. Sijacki^{12a}, O. Silbert¹⁷², J. Silva^{124a}, Y. Silver¹⁵³,
 D. Silverstein¹⁴³, S.B. Silverstein^{146a}, V. Simak¹²⁷, O. Simard¹³⁶, Lj. Simic^{12a}, S. Simion¹¹⁵,
 E. Simioni⁸¹, B. Simmons⁷⁷, R. Simoniello^{89a,89b}, M. Simonyan³⁵, P. Sinervo¹⁵⁸,
 N.B. Sinev¹¹⁴, V. Sipica¹⁴¹, G. Siragusa¹⁷⁴, A. Sircar²⁴, A.N. Sisakyan⁶⁴,
 S.Yu. Sivoklokov⁹⁷, J. Sjölin^{146a,146b}, T.B. Sjrursen¹³, L.A. Skinnari¹⁴, H.P. Skottowe⁵⁷,

K. Skovpen¹⁰⁷, P. Skubic¹¹¹, M. Slater¹⁷, T. Slavicek¹²⁷, K. Sliwa¹⁶¹, V. Smakhtin¹⁷²,
 B.H. Smart⁴⁵, S.Yu. Smirnov⁹⁶, Y. Smirnov⁹⁶, L.N. Smirnova⁹⁷, O. Smirnova⁷⁹,
 B.C. Smith⁵⁷, D. Smith¹⁴³, K.M. Smith⁵³, M. Smizanska⁷¹, K. Smolek¹²⁷, A.A. Snesev⁹⁴,
 S.W. Snow⁸², J. Snow¹¹¹, S. Snyder²⁴, R. Sobie^{169,k}, J. Sodomka¹²⁷, A. Soffer¹⁵³,
 C.A. Solans¹⁶⁷, M. Solar¹²⁷, J. Solc¹²⁷, E.Yu. Soldatov⁹⁶, U. Soldevila¹⁶⁷,
 E. Solfaroli Camillocci^{132a,132b}, A.A. Solodkov¹²⁸, O.V. Solovyanov¹²⁸, N. Soni²,
 V. Sopko¹²⁷, B. Sopko¹²⁷, M. Sosebee⁷, R. Soualah^{164a,164c}, A. Soukharev¹⁰⁷,
 S. Spagnolo^{72a,72b}, F. Spanò⁷⁶, R. Spighi^{19a}, G. Spigo²⁹, F. Spila^{132a,132b}, R. Spiwox²⁹,
 M. Spousta¹²⁶, T. Spreitzer¹⁵⁸, B. Spurlock⁷, R.D. St. Denis⁵³, J. Stahlman¹²⁰,
 R. Stamen^{58a}, E. Stanecka³⁸, R.W. Stanek⁵, C. Stanescu^{134a}, M. Stanescu-Bellu⁴¹,
 S. Stapnes¹¹⁷, E.A. Starchenko¹²⁸, J. Stark⁵⁵, P. Staroba¹²⁵, P. Starovoitov⁴¹,
 R. Staszewski³⁸, A. Staude⁹⁸, P. Stavina^{144a}, G. Steele⁵³, P. Steinbach⁴³, P. Steinberg²⁴,
 I. Stekl¹²⁷, B. Stelzer¹⁴², H.J. Stelzer⁸⁸, O. Stelzer-Chilton^{159a}, H. Stenzel⁵², S. Stern⁹⁹,
 G.A. Stewart²⁹, J.A. Stillings²⁰, M.C. Stockton⁸⁵, K. Stoerig⁴⁸, G. Stoicea^{25a}, S. Stonjek⁹⁹,
 P. Strachota¹²⁶, A.R. Stradling⁷, A. Straessner⁴³, J. Strandberg¹⁴⁷, S. Strandberg^{146a,146b},
 A. Strandlie¹¹⁷, M. Strang¹⁰⁹, E. Strauss¹⁴³, M. Strauss¹¹¹, P. Strizenec^{144b}, R. Ströhmer¹⁷⁴,
 D.M. Strom¹¹⁴, J.A. Strong^{76,*}, R. Stroynowski³⁹, J. Strube¹²⁹, B. Stugu¹³, I. Stumer^{24,*},
 J. Stupak¹⁴⁸, P. Sturm¹⁷⁵, N.A. Styles⁴¹, D.A. Soh^{151,w}, D. Su¹⁴³, HS. Subramania²,
 A. Succurro¹¹, Y. Sugaya¹¹⁶, C. Suhr¹⁰⁶, M. Suk¹²⁶, V.V. Sulin⁹⁴, S. Sultansoy^{3d},
 T. Sumida⁶⁷, X. Sun⁵⁵, J.E. Sundermann⁴⁸, K. Suruliz¹³⁹, G. Susinno^{36a,36b},
 M.R. Sutton¹⁴⁹, Y. Suzuki⁶⁵, Y. Suzuki⁶⁶, M. Svatos¹²⁵, S. Swedish¹⁶⁸, I. Sykora^{144a},
 T. Sykora¹²⁶, J. Sánchez¹⁶⁷, D. Ta¹⁰⁵, K. Tackmann⁴¹, A. Taffard¹⁶³, R. Tafirout^{159a},
 N. Taiblum¹⁵³, Y. Takahashi¹⁰¹, H. Takai²⁴, R. Takashima⁶⁸, H. Takeda⁶⁶, T. Takeshita¹⁴⁰,
 Y. Takubo⁶⁵, M. Talby⁸³, A. Talyshev^{107,f}, M.C. Tamsett²⁴, J. Tanaka¹⁵⁵, R. Tanaka¹¹⁵,
 S. Tanaka¹³¹, S. Tanaka⁶⁵, A.J. Tanasijczuk¹⁴², K. Tani⁶⁶, N. Tannoury⁸³, S. Tapprogge⁸¹,
 D. Tardif¹⁵⁸, S. Tarem¹⁵², F. Tarrade²⁸, G.F. Tartarelli^{89a}, P. Tas¹²⁶, M. Tasevsky¹²⁵,
 E. Tassi^{36a,36b}, M. Tatarkhanov¹⁴, Y. Tayalati^{135d}, C. Taylor⁷⁷, F.E. Taylor⁹²,
 G.N. Taylor⁸⁶, W. Taylor^{159b}, M. Teinturier¹¹⁵, M. Teixeira Dias Castanheira⁷⁵,
 P. Teixeira-Dias⁷⁶, K.K. Temming⁴⁸, H. Ten Kate²⁹, P.K. Teng¹⁵¹, S. Terada⁶⁵,
 K. Terashi¹⁵⁵, J. Terron⁸⁰, M. Testa⁴⁷, R.J. Teuscher^{158,k}, J. Therhaag²⁰,
 T. Theveneaux-Pelzer⁷⁸, S. Thoma⁴⁸, J.P. Thomas¹⁷, E.N. Thompson³⁴, P.D. Thompson¹⁷,
 P.D. Thompson¹⁵⁸, A.S. Thompson⁵³, L.A. Thomsen³⁵, E. Thomson¹²⁰, M. Thomson²⁷,
 R.P. Thun⁸⁷, F. Tian³⁴, M.J. Tibbetts¹⁴, T. Tic¹²⁵, V.O. Tikhomirov⁹⁴,
 Y.A. Tikhonov^{107,f}, S. Timoshenko⁹⁶, P. Tipton¹⁷⁶, F.J. Tique Aires Viegas²⁹,
 S. Tisserant⁸³, T. Todorov⁴, S. Todorova-Nova¹⁶¹, B. Toggerson¹⁶³, J. Tojo⁶⁹, S. Tokár^{144a},
 K. Tokushuku⁶⁵, K. Tollefson⁸⁸, M. Tomoto¹⁰¹, L. Tompkins³⁰, K. Toms¹⁰³, A. Tonoyan¹³,
 C. Topfel¹⁶, N.D. Topilin⁶⁴, I. Torchiani²⁹, E. Torrence¹¹⁴, H. Torres⁷⁸, E. Torró Pastor¹⁶⁷,
 J. Toth^{83,ad}, F. Touchard⁸³, D.R. Tovey¹³⁹, T. Trefzger¹⁷⁴, L. Tremblet²⁹, A. Tricoli²⁹,
 I.M. Trigger^{159a}, S. Trincaz-Duvold⁷⁸, M.F. Tripiana⁷⁰, W. Trischuk¹⁵⁸, B. Trocme⁵⁵,
 C. Troncon^{89a}, M. Trotter-McDonald¹⁴², M. Trzebinski³⁸, A. Trzupek³⁸, C. Tsarouchas²⁹,
 J.C-L. Tseng¹¹⁸, M. Tsiakiris¹⁰⁵, P.V. Tsiareshka⁹⁰, D. Tsionou^{4,ah}, G. Tsipolitis⁹,
 V. Tsiskaridze⁴⁸, E.G. Tskhadadze^{51a}, I.I. Tsukerman⁹⁵, V. Tsulaia¹⁴, J.-W. Tsung²⁰,
 S. Tsuno⁶⁵, D. Tsybychev¹⁴⁸, A. Tua¹³⁹, A. Tudorache^{25a}, V. Tudorache^{25a}, J.M. Tuggle³⁰,

M. Turala³⁸, D. Turecek¹²⁷, I. Turk Cakin^{3e}, E. Turlay¹⁰⁵, R. Turra^{89a,89b}, P.M. Tuts³⁴,
A. Tykhonov⁷⁴, M. Tylmad^{146a,146b}, M. Tyndel¹²⁹, G. Tzanakos⁸, K. Uchida²⁰, I. Ueda¹⁵⁵,
R. Ueno²⁸, M. Ugland¹³, M. Uhlenbrock²⁰, M. Uhrmacher⁵⁴, F. Ukegawa¹⁶⁰, G. Unal²⁹,
A. Undrus²⁴, G. Unel¹⁶³, Y. Unno⁶⁵, D. Urbaniec³⁴, G. Usai⁷, M. Uslenghi^{119a,119b},
L. Vacavant⁸³, V. Vacek¹²⁷, B. Vachon⁸⁵, S. Vahsen¹⁴, J. Valenta¹²⁵, P. Valente^{132a},
S. Valentinetti^{19a,19b}, A. Valero¹⁶⁷, S. Valkar¹²⁶, E. Valladolid Gallego¹⁶⁷, S. Vallecorsa¹⁵²,
J.A. Valls Ferrer¹⁶⁷, H. van der Graaf¹⁰⁵, E. van der Kraaij¹⁰⁵, R. Van Der Leeuw¹⁰⁵,
E. van der Poel¹⁰⁵, D. van der Ster²⁹, N. van Eldik²⁹, P. van Gemmeren⁵, I. van Vulpen¹⁰⁵,
M. Vanadia⁹⁹, W. Vandelli²⁹, A. Vaniachine⁵, P. Vankov⁴¹, F. Vannucci⁷⁸, R. Vari^{132a},
T. Varol⁸⁴, D. Varouchas¹⁴, A. Vartapetian⁷, K.E. Varvell¹⁵⁰, V.I. Vassilakopoulos⁵⁶,
F. Vazeille³³, T. Vazquez Schroeder⁵⁴, G. Vegni^{89a,89b}, J.J. Veillet¹¹⁵, F. Veloso^{124a},
R. Veness²⁹, S. Veneziano^{132a}, A. Ventura^{72a,72b}, D. Ventura⁸⁴, M. Venturi⁴⁸, N. Venturi¹⁵⁸,
V. Vercesi^{119a}, M. Verducci¹³⁸, W. Verkerke¹⁰⁵, J.C. Vermeulen¹⁰⁵, A. Vest⁴³,
M.C. Vetterli^{142,d}, I. Vichou¹⁶⁵, T. Vickey^{145b,ai}, O.E. Vickey Boeriu^{145b},
G.H.A. Viehhauser¹¹⁸, S. Viel¹⁶⁸, M. Villa^{19a,19b}, M. Villaplana Perez¹⁶⁷, E. Vilucchi⁴⁷,
M.G. Vincter²⁸, E. Vinek²⁹, V.B. Vinogradov⁶⁴, M. Virchaux^{136,*}, J. Virzi¹⁴, O. Vitells¹⁷²,
M. Viti⁴¹, I. Vivarelli⁴⁸, F. Vives Vaque², S. Vlachos⁹, D. Vladoiu⁹⁸, M. Vlasak¹²⁷,
A. Vogel²⁰, P. Vokac¹²⁷, G. Volpi⁴⁷, M. Volpi⁸⁶, G. Volpini^{89a}, H. von der Schmitt⁹⁹,
J. von Loeben⁹⁹, H. von Radziewski⁴⁸, E. von Toerne²⁰, V. Vorobel¹²⁶, V. Vorwerk¹¹,
M. Vos¹⁶⁷, R. Voss²⁹, T.T. Voss¹⁷⁵, J.H. Vossebeld⁷³, N. Vranjes¹³⁶,
M. Vranjes Milosavljevic¹⁰⁵, V. Vrba¹²⁵, M. Vreeswijk¹⁰⁵, T. Vu Anh⁴⁸, R. Vuillermet²⁹,
I. Vukotic¹¹⁵, W. Wagner¹⁷⁵, P. Wagner¹²⁰, H. Wahlen¹⁷⁵, S. Wahrmund⁴³,
J. Wakabayashi¹⁰¹, S. Walch⁸⁷, J. Walder⁷¹, R. Walker⁹⁸, W. Walkowiak¹⁴¹, R. Wall¹⁷⁶,
P. Waller⁷³, C. Wang⁴⁴, H. Wang¹⁷³, H. Wang^{32b,aj}, J. Wang¹⁵¹, J. Wang⁵⁵, R. Wang¹⁰³,
S.M. Wang¹⁵¹, T. Wang²⁰, A. Warburton⁸⁵, C.P. Ward²⁷, M. Warsinsky⁴⁸, A. Washbrook⁴⁵,
C. Wasicki⁴¹, P.M. Watkins¹⁷, A.T. Watson¹⁷, I.J. Watson¹⁵⁰, M.F. Watson¹⁷, G. Watts¹³⁸,
S. Watts⁸², A.T. Waugh¹⁵⁰, B.M. Waugh⁷⁷, M. Weber¹²⁹, M.S. Weber¹⁶, P. Weber⁵⁴,
A.R. Weidberg¹¹⁸, P. Weigell⁹⁹, J. Weingarten⁵⁴, C. Weiser⁴⁸, H. Wellenstein²²,
P.S. Wells²⁹, T. Wenaus²⁴, D. Wendland¹⁵, Z. Weng^{151,w}, T. Wengler²⁹, S. Wenig²⁹,
N. Wermes²⁰, M. Werner⁴⁸, P. Werner²⁹, M. Werth¹⁶³, M. Wessels^{58a}, J. Wetter¹⁶¹,
C. Weydert⁵⁵, K. Whalen²⁸, S.J. Wheeler-Ellis¹⁶³, A. White⁷, M.J. White⁸⁶,
S. White^{122a,122b}, S.R. Whitehead¹¹⁸, D. Whiteson¹⁶³, D. Whittington⁶⁰, F. Wicek¹¹⁵,
D. Wicke¹⁷⁵, F.J. Wickens¹²⁹, W. Wiedenmann¹⁷³, M. Wielers¹²⁹, P. Wienemann²⁰,
C. Wiglesworth⁷⁵, L.A.M. Wiik-Fuchs⁴⁸, P.A. Wijeratne⁷⁷, A. Wildauer¹⁶⁷, M.A. Wildt^{41,s},
I. Wilhelm¹²⁶, H.G. Wilkens²⁹, J.Z. Will⁹⁸, E. Williams³⁴, H.H. Williams¹²⁰, W. Willis³⁴,
S. Willocq⁸⁴, J.A. Wilson¹⁷, M.G. Wilson¹⁴³, A. Wilson⁸⁷, I. Wingerter-Seez⁴,
S. Winkelmann⁴⁸, F. Winklmeier²⁹, M. Wittgen¹⁴³, S.J. Wollstadt⁸¹, M.W. Wolter³⁸,
H. Wolters^{124a,h}, W.C. Wong⁴⁰, G. Wooden⁸⁷, B.K. Wosiek³⁸, J. Wotschack²⁹,
M.J. Woudstra⁸², K.W. Wozniak³⁸, K. Wraight⁵³, C. Wright⁵³, M. Wright⁵³, B. Wrona⁷³,
S.L. Wu¹⁷³, X. Wu⁴⁹, Y. Wu^{32b,ak}, E. Wulf³⁴, B.M. Wynne⁴⁵, S. Xella³⁵, M. Xiao¹³⁶,
S. Xie⁴⁸, C. Xu^{32b,z}, D. Xu¹³⁹, B. Yabsley¹⁵⁰, S. Yacoob^{145b}, M. Yamada⁶⁵,
H. Yamaguchi¹⁵⁵, A. Yamamoto⁶⁵, K. Yamamoto⁶³, S. Yamamoto¹⁵⁵, T. Yamamura¹⁵⁵,
T. Yamanaka¹⁵⁵, J. Yamaoka⁴⁴, T. Yamazaki¹⁵⁵, Y. Yamazaki⁶⁶, Z. Yan²¹, H. Yang⁸⁷,

U.K. Yang⁸², Y. Yang⁶⁰, Z. Yang^{146a,146b}, S. Yanush⁹¹, L. Yao^{32a}, Y. Yao¹⁴, Y. Yasu⁶⁵, G.V. Ybeles Smit¹³⁰, J. Ye³⁹, S. Ye²⁴, M. Yilmaz^{3c}, R. Yoosoofmiya¹²³, K. Yorita¹⁷¹, R. Yoshida⁵, C. Young¹⁴³, C.J. Young¹¹⁸, S. Youssef²¹, D. Yu²⁴, J. Yu⁷, J. Yu¹¹², L. Yuan⁶⁶, A. Yurkewicz¹⁰⁶, B. Zabinski³⁸, R. Zaidan⁶², A.M. Zaitsev¹²⁸, Z. Zajacova²⁹, L. Zanello^{132a,132b}, A. Zaytsev¹⁰⁷, C. Zeitnitz¹⁷⁵, M. Zeman¹²⁵, A. Zemla³⁸, C. Zender²⁰, O. Zenin¹²⁸, T. Ženiš^{144a}, Z. Zinonos^{122a,122b}, S. Zenz¹⁴, D. Zerwas¹¹⁵, G. Zevi della Porta⁵⁷, Z. Zhan^{32d}, D. Zhang^{32b,aj}, H. Zhang⁸⁸, J. Zhang⁵, X. Zhang^{32d}, Z. Zhang¹¹⁵, L. Zhao¹⁰⁸, T. Zhao¹³⁸, Z. Zhao^{32b}, A. Zhemchugov⁶⁴, J. Zhong¹¹⁸, B. Zhou⁸⁷, N. Zhou¹⁶³, Y. Zhou¹⁵¹, C.G. Zhu^{32d}, H. Zhu⁴¹, J. Zhu⁸⁷, Y. Zhu^{32b}, X. Zhuang⁹⁸, V. Zhuravlov⁹⁹, D. Zieminska⁶⁰, N.I. Zimin⁶⁴, R. Zimmermann²⁰, S. Zimmermann²⁰, S. Zimmermann⁴⁸, M. Ziolkowski¹⁴¹, R. Zitoun⁴, L. Živković³⁴, V.V. Zmouchko^{128,*}, G. Zobernig¹⁷³, A. Zoccoli^{19a,19b}, M. zur Nedden¹⁵, V. Zutshi¹⁰⁶, L. Zwalinski²⁹.

¹ University at Albany, Albany NY, United States of America

² Department of Physics, University of Alberta, Edmonton AB, Canada

³ ^(a)Department of Physics, Ankara University, Ankara; ^(b)Department of Physics, Dumlupinar University, Kutahya; ^(c)Department of Physics, Gazi University, Ankara; ^(d)Division of Physics, TOBB University of Economics and Technology, Ankara; ^(e)Turkish Atomic Energy Authority, Ankara, Turkey

⁴ LAPP, CNRS/IN2P3 and Université de Savoie, Annecy-le-Vieux, France

⁵ High Energy Physics Division, Argonne National Laboratory, Argonne IL, United States of America

⁶ Department of Physics, University of Arizona, Tucson AZ, United States of America

⁷ Department of Physics, The University of Texas at Arlington, Arlington TX, United States of America

⁸ Physics Department, University of Athens, Athens, Greece

⁹ Physics Department, National Technical University of Athens, Zografou, Greece

¹⁰ Institute of Physics, Azerbaijan Academy of Sciences, Baku, Azerbaijan

¹¹ Institut de Física d'Altes Energies and Departament de Física de la Universitat Autònoma de Barcelona and ICREA, Barcelona, Spain

¹² ^(a)Institute of Physics, University of Belgrade, Belgrade; ^(b)Vinca Institute of Nuclear Sciences, University of Belgrade, Belgrade, Serbia

¹³ Department for Physics and Technology, University of Bergen, Bergen, Norway

¹⁴ Physics Division, Lawrence Berkeley National Laboratory and University of California, Berkeley CA, United States of America

¹⁵ Department of Physics, Humboldt University, Berlin, Germany

¹⁶ Albert Einstein Center for Fundamental Physics and Laboratory for High Energy Physics, University of Bern, Bern, Switzerland

¹⁷ School of Physics and Astronomy, University of Birmingham, Birmingham, United Kingdom

¹⁸ ^(a)Department of Physics, Bogazici University, Istanbul; ^(b)Division of Physics, Dogus University, Istanbul; ^(c)Department of Physics Engineering, Gaziantep University, Gaziantep; ^(d)Department of Physics, Istanbul Technical University, Istanbul, Turkey

- ¹⁹ ^(a)INFN Sezione di Bologna; ^(b)Dipartimento di Fisica, Università di Bologna, Bologna, Italy
- ²⁰ Physikalisches Institut, University of Bonn, Bonn, Germany
- ²¹ Department of Physics, Boston University, Boston MA, United States of America
- ²² Department of Physics, Brandeis University, Waltham MA, United States of America
- ²³ ^(a)Universidade Federal do Rio De Janeiro COPPE/EE/IF, Rio de Janeiro; ^(b)Federal University of Juiz de Fora (UFJF), Juiz de Fora; ^(c)Federal University of Sao Joao del Rei (UFSJ), Sao Joao del Rei; ^(d)Instituto de Fisica, Universidade de Sao Paulo, Sao Paulo, Brazil
- ²⁴ Physics Department, Brookhaven National Laboratory, Upton NY, United States of America
- ²⁵ ^(a)National Institute of Physics and Nuclear Engineering, Bucharest; ^(b)University Politehnica Bucharest, Bucharest; ^(c)West University in Timisoara, Timisoara, Romania
- ²⁶ Departamento de Física, Universidad de Buenos Aires, Buenos Aires, Argentina
- ²⁷ Cavendish Laboratory, University of Cambridge, Cambridge, United Kingdom
- ²⁸ Department of Physics, Carleton University, Ottawa ON, Canada
- ²⁹ CERN, Geneva, Switzerland
- ³⁰ Enrico Fermi Institute, University of Chicago, Chicago IL, United States of America
- ³¹ ^(a)Departamento de Física, Pontificia Universidad Católica de Chile, Santiago; ^(b)Departamento de Física, Universidad Técnica Federico Santa María, Valparaíso, Chile
- ³² ^(a)Institute of High Energy Physics, Chinese Academy of Sciences, Beijing; ^(b)Department of Modern Physics, University of Science and Technology of China, Anhui; ^(c)Department of Physics, Nanjing University, Jiangsu; ^(d)School of Physics, Shandong University, Shandong, China
- ³³ Laboratoire de Physique Corpusculaire, Clermont Université and Université Blaise Pascal and CNRS/IN2P3, Aubiere Cedex, France
- ³⁴ Nevis Laboratory, Columbia University, Irvington NY, United States of America
- ³⁵ Niels Bohr Institute, University of Copenhagen, Kobenhavn, Denmark
- ³⁶ ^(a)INFN Gruppo Collegato di Cosenza; ^(b)Dipartimento di Fisica, Università della Calabria, Arcavata di Rende, Italy
- ³⁷ AGH University of Science and Technology, Faculty of Physics and Applied Computer Science, Krakow, Poland
- ³⁸ The Henryk Niewodniczanski Institute of Nuclear Physics, Polish Academy of Sciences, Krakow, Poland
- ³⁹ Physics Department, Southern Methodist University, Dallas TX, United States of America
- ⁴⁰ Physics Department, University of Texas at Dallas, Richardson TX, United States of America
- ⁴¹ DESY, Hamburg and Zeuthen, Germany
- ⁴² Institut für Experimentelle Physik IV, Technische Universität Dortmund, Dortmund, Germany
- ⁴³ Institut für Kern- und Teilchenphysik, Technical University Dresden, Dresden, Germany
- ⁴⁴ Department of Physics, Duke University, Durham NC, United States of America

- ⁴⁵ SUPA - School of Physics and Astronomy, University of Edinburgh, Edinburgh, United Kingdom
- ⁴⁶ Fachhochschule Wiener Neustadt, Johannes Gutenbergstrasse 3 2700 Wiener Neustadt, Austria
- ⁴⁷ INFN Laboratori Nazionali di Frascati, Frascati, Italy
- ⁴⁸ Fakultät für Mathematik und Physik, Albert-Ludwigs-Universität, Freiburg i.Br., Germany
- ⁴⁹ Section de Physique, Université de Genève, Geneva, Switzerland
- ⁵⁰ ^(a)INFN Sezione di Genova; ^(b)Dipartimento di Fisica, Università di Genova, Genova, Italy
- ⁵¹ ^(a)E.Andronikashvili Institute of Physics, Tbilisi State University, Tbilisi; ^(b)High Energy Physics Institute, Tbilisi State University, Tbilisi, Georgia
- ⁵² II Physikalisches Institut, Justus-Liebig-Universität Giessen, Giessen, Germany
- ⁵³ SUPA - School of Physics and Astronomy, University of Glasgow, Glasgow, United Kingdom
- ⁵⁴ II Physikalisches Institut, Georg-August-Universität, Göttingen, Germany
- ⁵⁵ Laboratoire de Physique Subatomique et de Cosmologie, Université Joseph Fourier and CNRS/IN2P3 and Institut National Polytechnique de Grenoble, Grenoble, France
- ⁵⁶ Department of Physics, Hampton University, Hampton VA, United States of America
- ⁵⁷ Laboratory for Particle Physics and Cosmology, Harvard University, Cambridge MA, United States of America
- ⁵⁸ ^(a)Kirchhoff-Institut für Physik, Ruprecht-Karls-Universität Heidelberg, Heidelberg; ^(b)Physikalisches Institut, Ruprecht-Karls-Universität Heidelberg, Heidelberg; ^(c)ZITI Institut für technische Informatik, Ruprecht-Karls-Universität Heidelberg, Mannheim, Germany
- ⁵⁹ Faculty of Applied Information Science, Hiroshima Institute of Technology, Hiroshima, Japan
- ⁶⁰ Department of Physics, Indiana University, Bloomington IN, United States of America
- ⁶¹ Institut für Astro- und Teilchenphysik, Leopold-Franzens-Universität, Innsbruck, Austria
- ⁶² University of Iowa, Iowa City IA, United States of America
- ⁶³ Department of Physics and Astronomy, Iowa State University, Ames IA, United States of America
- ⁶⁴ Joint Institute for Nuclear Research, JINR Dubna, Dubna, Russia
- ⁶⁵ KEK, High Energy Accelerator Research Organization, Tsukuba, Japan
- ⁶⁶ Graduate School of Science, Kobe University, Kobe, Japan
- ⁶⁷ Faculty of Science, Kyoto University, Kyoto, Japan
- ⁶⁸ Kyoto University of Education, Kyoto, Japan
- ⁶⁹ Department of Physics, Kyushu University, Fukuoka, Japan
- ⁷⁰ Instituto de Física La Plata, Universidad Nacional de La Plata and CONICET, La Plata, Argentina
- ⁷¹ Physics Department, Lancaster University, Lancaster, United Kingdom
- ⁷² ^(a)INFN Sezione di Lecce; ^(b)Dipartimento di Matematica e Fisica, Università del Salento, Lecce, Italy

- ⁷³ Oliver Lodge Laboratory, University of Liverpool, Liverpool, United Kingdom
- ⁷⁴ Department of Physics, Jožef Stefan Institute and University of Ljubljana, Ljubljana, Slovenia
- ⁷⁵ School of Physics and Astronomy, Queen Mary University of London, London, United Kingdom
- ⁷⁶ Department of Physics, Royal Holloway University of London, Surrey, United Kingdom
- ⁷⁷ Department of Physics and Astronomy, University College London, London, United Kingdom
- ⁷⁸ Laboratoire de Physique Nucléaire et de Hautes Energies, UPMC and Université Paris-Diderot and CNRS/IN2P3, Paris, France
- ⁷⁹ Fysiska institutionen, Lunds universitet, Lund, Sweden
- ⁸⁰ Departamento de Física Teórica C-15, Universidad Autónoma de Madrid, Madrid, Spain
- ⁸¹ Institut für Physik, Universität Mainz, Mainz, Germany
- ⁸² School of Physics and Astronomy, University of Manchester, Manchester, United Kingdom
- ⁸³ CPPM, Aix-Marseille Université and CNRS/IN2P3, Marseille, France
- ⁸⁴ Department of Physics, University of Massachusetts, Amherst MA, United States of America
- ⁸⁵ Department of Physics, McGill University, Montreal QC, Canada
- ⁸⁶ School of Physics, University of Melbourne, Victoria, Australia
- ⁸⁷ Department of Physics, The University of Michigan, Ann Arbor MI, United States of America
- ⁸⁸ Department of Physics and Astronomy, Michigan State University, East Lansing MI, United States of America
- ⁸⁹ ^(a)INFN Sezione di Milano; ^(b)Dipartimento di Fisica, Università di Milano, Milano, Italy
- ⁹⁰ B.I. Stepanov Institute of Physics, National Academy of Sciences of Belarus, Minsk, Republic of Belarus
- ⁹¹ National Scientific and Educational Centre for Particle and High Energy Physics, Minsk, Republic of Belarus
- ⁹² Department of Physics, Massachusetts Institute of Technology, Cambridge MA, United States of America
- ⁹³ Group of Particle Physics, University of Montreal, Montreal QC, Canada
- ⁹⁴ P.N. Lebedev Institute of Physics, Academy of Sciences, Moscow, Russia
- ⁹⁵ Institute for Theoretical and Experimental Physics (ITEP), Moscow, Russia
- ⁹⁶ Moscow Engineering and Physics Institute (MEPhI), Moscow, Russia
- ⁹⁷ Skobeltsyn Institute of Nuclear Physics, Lomonosov Moscow State University, Moscow, Russia
- ⁹⁸ Fakultät für Physik, Ludwig-Maximilians-Universität München, München, Germany
- ⁹⁹ Max-Planck-Institut für Physik (Werner-Heisenberg-Institut), München, Germany
- ¹⁰⁰ Nagasaki Institute of Applied Science, Nagasaki, Japan
- ¹⁰¹ Graduate School of Science, Nagoya University, Nagoya, Japan
- ¹⁰² ^(a)INFN Sezione di Napoli; ^(b)Dipartimento di Scienze Fisiche, Università di Napoli, Napoli, Italy

- ¹⁰³ Department of Physics and Astronomy, University of New Mexico, Albuquerque NM, United States of America
- ¹⁰⁴ Institute for Mathematics, Astrophysics and Particle Physics, Radboud University Nijmegen/Nikhef, Nijmegen, Netherlands
- ¹⁰⁵ Nikhef National Institute for Subatomic Physics and University of Amsterdam, Amsterdam, Netherlands
- ¹⁰⁶ Department of Physics, Northern Illinois University, DeKalb IL, United States of America
- ¹⁰⁷ Budker Institute of Nuclear Physics, SB RAS, Novosibirsk, Russia
- ¹⁰⁸ Department of Physics, New York University, New York NY, United States of America
- ¹⁰⁹ Ohio State University, Columbus OH, United States of America
- ¹¹⁰ Faculty of Science, Okayama University, Okayama, Japan
- ¹¹¹ Homer L. Dodge Department of Physics and Astronomy, University of Oklahoma, Norman OK, United States of America
- ¹¹² Department of Physics, Oklahoma State University, Stillwater OK, United States of America
- ¹¹³ Palacký University, RCPTM, Olomouc, Czech Republic
- ¹¹⁴ Center for High Energy Physics, University of Oregon, Eugene OR, United States of America
- ¹¹⁵ LAL, Université Paris-Sud and CNRS/IN2P3, Orsay, France
- ¹¹⁶ Graduate School of Science, Osaka University, Osaka, Japan
- ¹¹⁷ Department of Physics, University of Oslo, Oslo, Norway
- ¹¹⁸ Department of Physics, Oxford University, Oxford, United Kingdom
- ¹¹⁹ ^(a)INFN Sezione di Pavia; ^(b)Dipartimento di Fisica, Università di Pavia, Pavia, Italy
- ¹²⁰ Department of Physics, University of Pennsylvania, Philadelphia PA, United States of America
- ¹²¹ Petersburg Nuclear Physics Institute, Gatchina, Russia
- ¹²² ^(a)INFN Sezione di Pisa; ^(b)Dipartimento di Fisica E. Fermi, Università di Pisa, Pisa, Italy
- ¹²³ Department of Physics and Astronomy, University of Pittsburgh, Pittsburgh PA, United States of America
- ¹²⁴ ^(a)Laboratorio de Instrumentacao e Fisica Experimental de Particulas - LIP, Lisboa, Portugal; ^(b)Departamento de Fisica Teorica y del Cosmos and CAFPE, Universidad de Granada, Granada, Spain
- ¹²⁵ Institute of Physics, Academy of Sciences of the Czech Republic, Praha, Czech Republic
- ¹²⁶ Faculty of Mathematics and Physics, Charles University in Prague, Praha, Czech Republic
- ¹²⁷ Czech Technical University in Prague, Praha, Czech Republic
- ¹²⁸ State Research Center Institute for High Energy Physics, Protvino, Russia
- ¹²⁹ Particle Physics Department, Rutherford Appleton Laboratory, Didcot, United Kingdom
- ¹³⁰ Physics Department, University of Regina, Regina SK, Canada
- ¹³¹ Ritsumeikan University, Kusatsu, Shiga, Japan

- ¹³² ^(a)INFN Sezione di Roma I; ^(b)Dipartimento di Fisica, Università La Sapienza, Roma, Italy
- ¹³³ ^(a)INFN Sezione di Roma Tor Vergata; ^(b)Dipartimento di Fisica, Università di Roma Tor Vergata, Roma, Italy
- ¹³⁴ ^(a)INFN Sezione di Roma Tre; ^(b)Dipartimento di Fisica, Università Roma Tre, Roma, Italy
- ¹³⁵ ^(a)Faculté des Sciences Ain Chock, Réseau Universitaire de Physique des Hautes Energies - Université Hassan II, Casablanca; ^(b)Centre National de l'Energie des Sciences Techniques Nucleaires, Rabat; ^(c)Faculté des Sciences Semlalia, Université Cadi Ayyad, LPHEA-Marrakech; ^(d)Faculté des Sciences, Université Mohamed Premier and LPTPM, Oujda; ^(e)Faculté des sciences, Université Mohammed V-Agdal, Rabat, Morocco
- ¹³⁶ DSM/IRFU (Institut de Recherches sur les Lois Fondamentales de l'Univers), CEA Saclay (Commissariat a l'Energie Atomique), Gif-sur-Yvette, France
- ¹³⁷ Santa Cruz Institute for Particle Physics, University of California Santa Cruz, Santa Cruz CA, United States of America
- ¹³⁸ Department of Physics, University of Washington, Seattle WA, United States of America
- ¹³⁹ Department of Physics and Astronomy, University of Sheffield, Sheffield, United Kingdom
- ¹⁴⁰ Department of Physics, Shinshu University, Nagano, Japan
- ¹⁴¹ Fachbereich Physik, Universität Siegen, Siegen, Germany
- ¹⁴² Department of Physics, Simon Fraser University, Burnaby BC, Canada
- ¹⁴³ SLAC National Accelerator Laboratory, Stanford CA, United States of America
- ¹⁴⁴ ^(a)Faculty of Mathematics, Physics & Informatics, Comenius University, Bratislava; ^(b)Department of Subnuclear Physics, Institute of Experimental Physics of the Slovak Academy of Sciences, Kosice, Slovak Republic
- ¹⁴⁵ ^(a)Department of Physics, University of Johannesburg, Johannesburg; ^(b)School of Physics, University of the Witwatersrand, Johannesburg, South Africa
- ¹⁴⁶ ^(a)Department of Physics, Stockholm University; ^(b)The Oskar Klein Centre, Stockholm, Sweden
- ¹⁴⁷ Physics Department, Royal Institute of Technology, Stockholm, Sweden
- ¹⁴⁸ Departments of Physics & Astronomy and Chemistry, Stony Brook University, Stony Brook NY, United States of America
- ¹⁴⁹ Department of Physics and Astronomy, University of Sussex, Brighton, United Kingdom
- ¹⁵⁰ School of Physics, University of Sydney, Sydney, Australia
- ¹⁵¹ Institute of Physics, Academia Sinica, Taipei, Taiwan
- ¹⁵² Department of Physics, Technion: Israel Institute of Technology, Haifa, Israel
- ¹⁵³ Raymond and Beverly Sackler School of Physics and Astronomy, Tel Aviv University, Tel Aviv, Israel
- ¹⁵⁴ Department of Physics, Aristotle University of Thessaloniki, Thessaloniki, Greece
- ¹⁵⁵ International Center for Elementary Particle Physics and Department of Physics, The University of Tokyo, Tokyo, Japan
- ¹⁵⁶ Graduate School of Science and Technology, Tokyo Metropolitan University, Tokyo,

Japan

¹⁵⁷ Department of Physics, Tokyo Institute of Technology, Tokyo, Japan

¹⁵⁸ Department of Physics, University of Toronto, Toronto ON, Canada

¹⁵⁹ ^(a)TRIUMF, Vancouver BC; ^(b)Department of Physics and Astronomy, York University, Toronto ON, Canada

¹⁶⁰ Institute of Pure and Applied Sciences, University of Tsukuba, 1-1-1 Tennodai, Tsukuba, Ibaraki 305-8571, Japan

¹⁶¹ Science and Technology Center, Tufts University, Medford MA, United States of America

¹⁶² Centro de Investigaciones, Universidad Antonio Narino, Bogota, Colombia

¹⁶³ Department of Physics and Astronomy, University of California Irvine, Irvine CA, United States of America

¹⁶⁴ ^(a)INFN Gruppo Collegato di Udine; ^(b)ICTP, Trieste; ^(c)Dipartimento di Chimica, Fisica e Ambiente, Università di Udine, Udine, Italy

¹⁶⁵ Department of Physics, University of Illinois, Urbana IL, United States of America

¹⁶⁶ Department of Physics and Astronomy, University of Uppsala, Uppsala, Sweden

¹⁶⁷ Instituto de Física Corpuscular (IFIC) and Departamento de Física Atómica, Molecular y Nuclear and Departamento de Ingeniería Electrónica and Instituto de Microelectrónica de Barcelona (IMB-CNM), University of Valencia and CSIC, Valencia, Spain

¹⁶⁸ Department of Physics, University of British Columbia, Vancouver BC, Canada

¹⁶⁹ Department of Physics and Astronomy, University of Victoria, Victoria BC, Canada

¹⁷⁰ Department of Physics, University of Warwick, Coventry, United Kingdom

¹⁷¹ Waseda University, Tokyo, Japan

¹⁷² Department of Particle Physics, The Weizmann Institute of Science, Rehovot, Israel

¹⁷³ Department of Physics, University of Wisconsin, Madison WI, United States of America

¹⁷⁴ Fakultät für Physik und Astronomie, Julius-Maximilians-Universität, Würzburg, Germany

¹⁷⁵ Fachbereich C Physik, Bergische Universität Wuppertal, Wuppertal, Germany

¹⁷⁶ Department of Physics, Yale University, New Haven CT, United States of America

¹⁷⁷ Yerevan Physics Institute, Yerevan, Armenia

¹⁷⁸ Domaine scientifique de la Doua, Centre de Calcul CNRS/IN2P3, Villeurbanne Cedex, France

^a Also at Laboratório de Instrumentação e Física Experimental de Partículas - LIP, Lisboa, Portugal

^b Also at Faculdade de Ciências and CFNUL, Universidade de Lisboa, Lisboa, Portugal

^c Also at Particle Physics Department, Rutherford Appleton Laboratory, Didcot, United Kingdom

^d Also at TRIUMF, Vancouver BC, Canada

^e Also at Department of Physics, California State University, Fresno CA, United States of America

^f Also at Novosibirsk State University, Novosibirsk, Russia

^g Also at Fermilab, Batavia IL, United States of America

^h Also at Department of Physics, University of Coimbra, Coimbra, Portugal

- ⁱ Also at Department of Physics, UASLP, San Luis Potosi, Mexico
- ^j Also at Università di Napoli Parthenope, Napoli, Italy
- ^k Also at Institute of Particle Physics (IPP), Canada
- ^l Also at Department of Physics, Middle East Technical University, Ankara, Turkey
- ^m Also at Louisiana Tech University, Ruston LA, United States of America
- ⁿ Also at Dep Fisica and CEFITEC of Faculdade de Ciencias e Tecnologia, Universidade Nova de Lisboa, Caparica, Portugal
- ^o Also at Department of Physics and Astronomy, University College London, London, United Kingdom
- ^p Also at Group of Particle Physics, University of Montreal, Montreal QC, Canada
- ^q Also at Department of Physics, University of Cape Town, Cape Town, South Africa
- ^r Also at Institute of Physics, Azerbaijan Academy of Sciences, Baku, Azerbaijan
- ^s Also at Institut für Experimentalphysik, Universität Hamburg, Hamburg, Germany
- ^t Also at Manhattan College, New York NY, United States of America
- ^u Also at School of Physics, Shandong University, Shandong, China
- ^v Also at CPPM, Aix-Marseille Université and CNRS/IN2P3, Marseille, France
- ^w Also at School of Physics and Engineering, Sun Yat-sen University, Guanzhou, China
- ^x Also at Academia Sinica Grid Computing, Institute of Physics, Academia Sinica, Taipei, Taiwan
- ^y Also at Dipartimento di Fisica, Università La Sapienza, Roma, Italy
- ^z Also at DSM/IRFU (Institut de Recherches sur les Lois Fondamentales de l'Univers), CEA Saclay (Commissariat à l'Énergie Atomique), Gif-sur-Yvette, France
- ^{aa} Also at Section de Physique, Université de Genève, Geneva, Switzerland
- ^{ab} Also at Departamento de Fisica, Universidade de Minho, Braga, Portugal
- ^{ac} Also at Department of Physics and Astronomy, University of South Carolina, Columbia SC, United States of America
- ^{ad} Also at Institute for Particle and Nuclear Physics, Wigner Research Centre for Physics, Budapest, Hungary
- ^{ae} Also at California Institute of Technology, Pasadena CA, United States of America
- ^{af} Also at Institute of Physics, Jagiellonian University, Krakow, Poland
- ^{ag} Also at LAL, Université Paris-Sud and CNRS/IN2P3, Orsay, France
- ^{ah} Also at Department of Physics and Astronomy, University of Sheffield, Sheffield, United Kingdom
- ^{ai} Also at Department of Physics, Oxford University, Oxford, United Kingdom
- ^{aj} Also at Institute of Physics, Academia Sinica, Taipei, Taiwan
- ^{ak} Also at Department of Physics, The University of Michigan, Ann Arbor MI, United States of America
- * Deceased